The Role of PRAJA2 in TSH- or Isoproterenol- Stimulated Lipolysis in Human Adipocytes

By

Arran McBride

Thesis submitted to the Department of Biochemistry, Microbiology and Immunology in partial fulfillment of the requirements for the degree of Master of Science

Department of Biochemistry, Microbiology and Immunology
Faculty of Medicine
University of Ottawa
Ottawa, Canada

ABSTRACT

Thyrotropin (TSH) binds to TSH receptors on thyrocytes to regulate development and growth of the thyroid gland, and to stimulate thyroid hormone production. Thyrotropin has also been shown to act in an extra-thyroidal fashion, and to engage TSH receptors on adipocytes to induce lipolysis, similar to the response seen by stimulation with β-adrenergic receptor agonists (i.e. isoproterenol). In both cell types, cAMP-dependent kinase (PKA) is activated. Recently, PRAJA2, a novel AKAP and E3 ubiquitin ligase that targets the regulatory subunits of PKA was identified. The ubiquitin-dependent proteasomal degradation of the PKA regulatory subunits, due to PKA- phosphorylated PRAJA2, prolongs the catalytic activity of PKA, as shown in neuroblastoma cells by Lignitto *et al*., 2011. In adipocytes, stimulated PKA activity is required for lipolysis. Additionally, PRAJA2 has been described to have increased expression in TSH-responsive, differentiated thyroid cancer cells when compared to anaplastic thyroid tumor (Cantara et al., 2012) The aim of this study was to characterize PRAJA2 and its potential influence on adipocyte lipolysis. These data confirm that TSH and isoproterenol stimulate lipolysis in primary human differentiated adipocytes. PRAJA2 is expressed at the mRNA and protein level in differentiated adipocytes, with no change following stimulation with TSH or isoproterenol. Stimulation with isoproterenol, but not TSH, increases PKA-dependent phosphorylation of a 122kDa (potentially PRAJA2) and 69kDa protein identified in PRAJA2 immunoprecipitates. These proteins may prove important for lipolytic signaling or other PRAJA2-dependent process in adipocytes. Experimentation was unable to identify interactions between PRAJA2 and PKAR2 in differentiated adipocytes; however further investigations are required before discounting this interaction. An attempt was made to knockdown PRAJA2 in this model, and measure effects on lipolytic response; however, this was unsuccessful. Taken together, PRAJA2 appears to

be phosphorylated following β-adrenergic stimulation in human adipocytes; however, further studies are needed to delineate the specific role of PRAJA2 in this human differentiated adipocyte model.

ACKNOWLEDGEMENTS

I would like to thank all our past and current lab members, collaborators and funding agencies for their help in completing this thesis.

- Firstly, I would like to recognize my thesis supervisor Dr. Alexander Sorisky. Sincerely, thank you first for taking me in and giving me the opportunity to complete my graduate studies at the University of Ottawa. You took a chance on me after a bit of a rough start. You always remained positive, encouraging, provided outstanding guidance and challenged me, keeping me on my toes at all times. Your support has been incredible and I can honestly say I have become a better scientist from working with you.

- A special thanks goes to research associate Dr. AnneMarie Gagnon. As the senior scientist in the lab you were there to train and guide me in all aspects of my project. Your patience and attentiveness allowed me grow as an independent scientist. Your ability to put up with my never-ending questions was instrumental in making my graduate studies in the Sorisky Lab such a success. I can definitely say it would have been a rough road without all of your help and encouragement.

- Thank you, Anne for keeping the lab stocked up with everything I needed, and providing technical help at all times.

- Thank you to everyone in the Sorisky lab for offering all your support, being so friendly and putting up with all my antics during my time in the lab.

Current Lab Members

- AnneMarie Gagnon
- Anne Landry
- Vian Peshdary
- David Felske
- Amanda Biernacka-Laroque
- Jason El Bilali

Collaborators and TAC Members

- Dr. Marry-Ellen Harper
- Dr. Mario Tiberi
- Patients and Surgeons of The Ottawa Hospital

Funding Sources

- University of Ottawa
- Ottawa Hospital Research Institute
- Ontario Graduate Scholarship
- Natural Sciences and Engineering Research Council of Canada
- Canadian Institutes of Health Research

TABLE OF CONTENTS

LIST OF ABBREVIATIONS

A
α-AR: α-Adrenergic Receptor
a.a: Amino Acid
ABHD5: α/β Hydrolase Domain-Containing Protein 5
AC: Adenylyl Cyclase
AKAP: A-Kinase Anchoring Protein
Akt: Protein Kinase B
AMP: Adenosine Monophosphate
AMPK: AMP-Activated Protein Kinase
ANOVA: Analysis of Variance
ANP: Atrial Natriuretic Peptide
Asp: Aspartic Acid
AT: Adipose Tissue
ATC: Anaplastic Thyroid Cancer
ATGL: Adipose Triglyceride Lipase
ATP: Adenosine Triphosphate

B
β-AR: β-Adrenergic Receptor
BAT: Brown Adipose Tissue
BCA: Bicinchoninic Acid
BN: Benign Nodules
BNP: Bone Natriuretic Peptide
BSA: Bovine Serum Albumin
bTSH: Bovine Thyroid Stimulating Hormone

C
C/EBP: CCAAT-Enhancer Binding Proteins
$CaCl_2$: Calcium Chloride
cAMP: Cyclic Adenosine Monophosphate
CDK5: Cyclin-Dependent Kinase 5
CDK5R1: Cyclin-Dependent Kinase 5 Regulatory Subunit 1
cDNA: Complimentary DNA
cGMP: Cyclic Guanosine Monophosphate
cm: Centimeter
cPKC: Conventional Protein Kinase C
CRC: Colorectal Cancer Cells
CREB: cAMP Response Element-Binding Protein
CVD: Cardiovascular Disease

D
DG: Diglyceride
DEPC: Diethylpyrocarbonate
dH_2O: Distilled Water

DOC: Deoxycholic Acid
DOX: Doxycycline
DMEM: Dulbecco's Modified Eagle Medium
DNA: Deoxyribonucleic Acid
dNTP: Deoxyribonucleotide Triphosphate

E
E1: Ubiquitin Activating Enzyme
E2: Ubiquitin Conjugating Enzyme
E3: Ubiquitin Ligase
EDTA: Ethylenediaminetetraacetic Acid
ERK1/2: Extracellular Signaling-Regulated Kinase 1 and 2 (p42/44)
EtOH: Ethanol

F
FABP4: Fatty Acid Binding Protein 4
FBS: Fetal Bovine Serum
f.c.: Final Concentration

G
g: Grams
G: Guage
G418: Geneticin
GC: Guanylyl Cyclase
GDP: Guanosine Diphosphate
Gi: Inhibitory G Protein
GLUT4: Glucose Transporter Type 4
GPCR: G Protein-Coupled Receptor
Gs: Stimulatory G Protein
GSIS: Glucose Stimulated Insulin Secretion
GTP: Guanosine Triphosphate

H
HBSS: HEPES Buffered Saline Soultion
HCl: Hydrochloric Acid
HEPES: 4-(2-hydroxyethyl)-1-piperazineethanesulfonic acid
HRP: Horseradish Peroxidase
hr(s): Hour(s)
His: Histidine
HPT: Hypothalamic-Pituitary-Thyroid
HSL: Hormone Sensitive Lipase

I
IBMX: 3-isobutyl-1-methylxanthine
i.e.: *id est* ("that is")
IGF-1R: Insulin-Like Growth Factor -1 Receptor
IgG: Immunoglobulin G

IL-1: Interleukin-1
IL-6: Interleukin-6
IOD: Integrated Optical Density
IP: Immunoprecipitation
IP3: Inositol Triphosphate

K
K_2HPO_4: Potassium Phosphate Dibasic
KCl: Potassium Cholride
kDa: Kilodalton
Kg: Kilogram
KOH: Potassium Hydroxide

L
L: Litre
LATS1/2: Large Tumor Suppressor
LB: Lysogeny Broth

M
µg: Microgram
µL: Microlitre
µm: Micrometer
µM: Micromolar
m: Meter
M: Molar (moles per litre)
MAPK: Mitogen-Activated Protein Kinase
MEM: Minimum Essential Media
mg: Milligram
MG: Monoglyceride
MGL: Monoglyceride Lipase
min: Minute
mL: Milliliters
mM: Millimolar
MMLV-RT: Maloney Murine Leukemia Virus Reverse Transcriptase
Mo: Mouse
MOB1: Mps One Binder 1
MOPS: 4-Morpholinepropanesulfonic Acid
MSC: Mesenchymal Stem Cells
mU: Miliunits

N
N_2: Diatomic Nitrogen
Na_2HPO_4: Soidum Phosphate Dibasic
NaCl: Sodium Chloride
NaF: Sodium Fluoride
NaPPi: Sodium Pyrophosphate
$NaVO_4$: Sodium Orthovanadate

NDAP1: Neurodap 1
NEAA: Non-Essential Amino Acid
NH_4Cl: Ammonium Chloride
nm: Nanometer
nM: Nanomolar
NP-40: Nonyl Phenoxypolyethyoxylethanol
NPR: Natriuretic Peptide Receptor
NPYR1: Neuropeptide Y Receptor 1
NT: Normal Tissue

P
PAGE: Polyacrylamide Gel Electrophoresis
PAT: Perilipin, Adipopholin and Tail-Interaction Protein
PBS: Phosphate Buffered Saline
PDE: Phosphodiesterase
PEG: Polyethylene glycol
pH: Power of Hydrogen
PIP2: Phosphatidylinositol 4,5-Bisphosphate
PJA2: PRAJA2 (gene)
PKA: Protein Kinase A
PKAC: Protein Kinase A Catalytic Subunit
PKAR2: Protein Kinase A Regulatory Subunit
PKB: Protein Kinase B
PKC: Protein Kinase C
PKG: Protein Kinase G
PLC: Phospholipase C
PLIN: Perlipin
PMSF: Phenylmethylsulfonyl Fluoride
PPAR: Peroxisome Proliferator-Activated Receptor
PTC: Papillary Thyroid Cancer

Q
qPCR: Quantitiative Real-Time Polymerase Chain Reaction

R
Rb: Rabbit
RFP: Red Fluorescent Protein
RNA: Ribonucleic Acid
rRNA: Ribosomal RNA
rpm: Revolutions Per Minute
RT: Room Temperature

S
SCH: Subclinical Hypothyroidism
S.D.: Standard Deviation
SDS: Sodium Dodecyl Sulfate
Ser: Serine

SIK2: Salt-Inducible Kinase 2
SREBP-1c: Sterol Regulatory Elelment-Binding Protein 1c
SVF: Stromal Vascular Fraction

T
T2D: Type-2 Diabetes
T3: Tri-iodothyronine
T4: Thyroxine
TCA: Trichloroacetic Acid
TE: Tris-EDTA
TG: Triglyceride
TGFβ: Transforming Growth Factor β
Thr: Threonine
TKR: Tyrosine Kinase Receptor
TNFα: Tumor Necrosis Factor Alpha
TRH: Thyrotropin Releasing Hormone
TSH: Thyroid Stimulating Hormone; Thyrotropin
TSHR: Thyroid Stimulating Hormone Receptor

U
U: Units
UPS: Ubiquitin-Proteasome System

V
V: Volts
VDCC: Voltage Dependent Calcium Channel
v/v: Volume Per Volume

W
WAT: White Adipose Tissue

X
X: Times
xg: Relative Centrifugal Force

Y
YAP: Yes-Associated Binding Protein 1

Numbers and Symbols
3': 3-prime
5': 5-prime
<: Less Than
>: Greater Than
^{o}C: Degrees Centigrade

LIST OF FIGURES AND ILLUSTRATIONS

1. INTRODUCTION

1.1 Adipose tissue

1.1.1 Adipose tissue composition and function

There are two types of adipose tissue within the human body: brown adipose tissue (BAT) and white adipose tissue (WAT). Briefly, BAT is highly dense with mitochondria and is implicated in thermogenesis, via fatty acid oxidation (Fedorenko et al., 2012). WAT functions as both the primary depot for storage of energy as well as an endocrine tissue. WAT stores lipids in the form of triglycerides (TG) and releases non-esterified fatty acids (NEFA) and glycerol via lipolysis (Rosen and Spiegelman, 2014). Together, BAT and WAT are important in maintaining whole body energy homeostasis through regulation of carbohydrate and lipid metabolism. WAT is the focus of this thesis.

WAT is composed of various cell types including but not limited to: adipocytes, preadipocytes (progenitors), immune cells (T cells, B cells and macrophages), mesenchymal stem cells (MSC) and endothelial cells. Adipocytes constitute 50-70% of the tissue while the stromal vascular fraction (SVF), composed of the other cell types listed, constitutes 20-40% of the tissue (Lee et al., 2013). This diverse network of cells works harmoniously to ensure the tissue functions properly. Problems begin to arise when the cellular network is disrupted, for example, with infiltration of immune cells (inflammation) or lack of vascular expansion (hypoxia and nutrient deficiency) (Pasarica et al., 2009).

The two main fat depots in the body are the subcutaneous (beneath the skin) and intra-abdominal visceral (around the organs) depots. Studies suggest that visceral fat deposition, compared to subcutaneous, has a strong association with cardiovascular disease (CVD) risk factors, including dyslipidemia and insulin resistance (Azuma et al., 2007; Fox et

al., 2007; Snijder et al., 2006; St-Pierre et al., 2007; Vega et al., 2006). This is often assessed by waist-to-hip circumference ratio (a measure of abdominal fat distribution) and, when high, is commonly referred to as apple-shaped obesity. Once the limit of lipid storage is reached in adipose tissue (AT), excess lipids may be ectopically stored in other tissues such as muscle, liver, heart and pancreas (which typically only contain small amounts of fat). This deposition causes tissue dysfunction and may lead to a variety of metabolic problems (Danforth, 2000).

Adipocytes store TG in lipid droplets, which occupy the majority of the cytoplasm. Adipose tissue can remodel itself in response to influxes of energy in the form of TG packaged in lipoproteins (Rosen and Spiegelman, 2014). To increase capacity to store energy within AT, there may be recruitment of preadipocytes for differentiation, creating more adipocytes (hyperplasia), or increased lipid storage within existing adipocytes (hypertrophy) (Arner and Spalding, 2010). Expansion via hyperplasia appears to maintain healthy metabolic function, since each cell contains a manageable amount of TG and is accompanied by expansion of the supporting matrix. Alternatively, hypertrophy is considered pathological expansion, and occurs with immune cell infiltration (M1 macrophages) resulting in inflammation and without angiogenic expansion resulting in a hypoxic state. These aspects of the hypertrophic state correlate with metabolic dysfunction such as insulin resistance (Arner and Spalding, 2010; Hauner, 2005).

1.1.2 Adipose tissue as an endocrine organ

As an endocrine organ WAT secretes a variety of peptide hormones (often referred to as adipokines). Leptin maintains body weight homeostasis through appetite suppression and the promotion of energy expenditure. Leptin is secreted by adipocytes and binds to leptin

receptors in the arcuate nucleus of the hypothalamus, blocking hunger signals (Leinninger et al., 2009). Adiponectin regulates glucose uptake and fatty acid breakdown by engaging its receptors in liver and skeletal muscle to increase activity of AMP-activated protein kinase (AMPK) and peroxisome proliferator-activated receptor α (PPARα). This promotes β-oxidation, glucose transporter type 4 (GLUT4) translocation to the plasma membrane (muscle) and decreased gluconeogenesis (liver). Adiponectin expression is inversely correlated to body weight, and has been linked to protection against insulin resistance and inflammation (Turer et al., 2011; Turer and Scherer, 2012). Resistin, released by WAT macrophages, is a risk factor for CVD, promoting inflammation and raising low-density lipoprotein levels, therefore disrupting cholesterol homeostasis. Additionally, increases in resistin have been linked to obesity and the subsequent development of insulin resistance (Kim et al., 2001; Steppan et al., 2001). Careful regulation of these adipose tissue-derived factors is important for controlling energy metabolism and, when disrupted, predisposes to obesity and type-2 diabetes (T2D).

Additionally, various immunomodulating agents are secreted by adipose tissue. Tumor necrosis factor alpha (TNFα), interleukin-1β (IL-1β) and interleukin-6 (IL-6) regulate many aspects of immune cell response. These cytokines are pro-inflammatory in response to infection (Fain et al., 2004). Additionally, their dysregulation in AT is linked to pathological inflammation seen in various disease states, such as obesity, insulin resistance and CVD (Hauner, 2005).

1.1.3 Adipose tissue dysfunction

AT relies on coordination between a diversity of cells and cellular signals to create a functional organ for energy homeostasis. Without this, metabolic complications (obesity,

T2D, CVD) may result (Lafontan, 2014). Factors that may cause dysfunctional AT include inflammation, pathological tissue expansion and dysregulation of lipid storage and release (Lafontan, 2014).

When adipose tissue cannot properly store and release lipids, harmful metabolic byproducts build-up in circulation. NEFA deposit in muscle and liver, and can generate harmful byproducts such as ceramides and acyl-CoA (Unger et al., 2010). Subsequently, these NEFA derivatives can activate inflammatory kinases (such as PKC, JNKs, IKK), leading to inhibitory phosphorylation responses that block insulin signaling (Guilherme et al., 2008).

Chronic low-grade inflammation is correlated with obesity. The regulation of various adipokines (TNFα, IL-6 and IL-1β) is disrupted, and this is associated with insulin resistance (Ouchi et al., 2011). Monocytes are recruited to inflamed AT, become macrophages, and form crown-like structures around adipocytes. This process acts in a positive-feedback manner such that more pro-inflammatory signals are produced, recruiting more immune cells (Cinti et al., 2005).

1.2 Lipolytic signaling in adipocytes

Lipolysis is the process through which TG are hydrolyzed into their component NEFA and glycerol backbone, which are released into the blood stream. NEFA bind to albumin for transport to various tissues, to be metabolized as an energy source via the Kreb's cycle or β-oxidation (Lafontan and Langin, 2009). Glycerol is converted to glyceraldehyde-3-phosphate in the liver and used as a substrate for either glycolysis or gluconeogenesis (Lafontan and Langin, 2009). Adipocyte lipolysis may be stimulated by lipolytic hormones

such as catecholamines, TSH, or ANP acting on their cognate receptors. Lipolysis is inhibited by insulin via the insulin receptor (Lafontan and Langin, 2009).

1.2.1 G protein-coupled receptors in mediation of lipolysis

GPCRs play an important role in signal transduction from external ligands to intracellular second messengers. GPCRs contain 7 α-helical transmembrane domains, 3 intracellular loops and 3 extracellular loops (Venkatakrishnan et al., 2013). Ligands for GPCRs include odors, pheromones, hormones and neurotransmitters. Often binding occurs via a cavity, which forms as the receptor adopts a barrel-like shape; however, extracellular binding to the N-terminal domain has also been reported (Lagerstrom and Schioth, 2008). Binding of a ligand to its GPCR causes a conformational change, in turn activating an associated G-protein by exchanging a GDP for GTP, inducing a signal cascade within the cell (Lagerstrom and Schioth, 2008). The signal is terminated by the hydrolysis of protein-bound GTP to GDP, and re-association of the G-protein with its receptor.

In adipocytes, lipolytic GPCRs activate the adenylyl cyclase (AC) system within the cell, increasing cAMP levels to stimulate lipolysis (Lafontan and Langin, 2009). When AC is activated by a G-stimulatory (Gs) protein, levels of cAMP rise within the cell and the lipolytic process is up-regulated. Conversely, G-inhibitory (Gi) protein inhibits AC, and attenuates these signals (Lafontan and Langin, 2009). It is a balance in cross-talk between GPCR stimulation of the AC system via Gs and inhibition of this process by Gi activation, that helps maintain homeostatic control of lipolysis within the cell.

Many Gs-coupled receptors have been documented and linked to lipolytic activation. However, their prevalence and action varies between species. In rodents, adrenocorticotropic hormone, α-melanocyte stimulating hormone and β-lipotropin hormone have been shown to

stimulate lipolysis via the melanocortin 2 receptor; but, these hormones show little to no response in human AT (Boston, 1999; Lafontan and Agid, 1979). Parathyroid hormone has been shown to activate lipolysis in humans via AC (Sinha et al., 1976; Taniguchi et al., 1987). β-adrenergic receptors (β-AR) and thyroid stimulating hormone receptors (TSHR) also act in this way in human AT and are the focus of this thesis.

Catecholamines are tyrosine-derived hormones released by the adrenal glands and the sympathetic nervous system. Under physiological conditions, they are active during times of energy need such as fasting or physical exercise. These hormones are also associated with the fight-or-flight response, increasing heart rate and blood pressure (Obeyesekere et al., 2013). Isoproterenol is a non-selective, synthetic agonist of $\beta_{1,2}$-AR, similar in structure to epinephrine. Due to its action as an agonistic of $\beta_{1,2}$-AR, isoproterenol stimulates lipolysis in human adipocytes via cAMP-mediated signaling (Mercader et al., 2011).

Three β-AR subtypes exist in humans (β_1, β_2, β_3), each of which is coupled to an α subunit of the Gs protein (Robidoux et al., 2004). β_1 and β_2 exist in many tissues including WAT and BAT and stimulate lipolysis in humans, as shown both *in vivo* and *in vitro* (Barbe et al., 1996; Mauriege et al., 1988). However, β_3-AR functionality has only been documented in WAT/BAT of rodents, rabbits, hamsters and dogs. Its role in human AT remains dubious and it does not contribute to catecholamine-induced lipolysis (Galitzky et al., 1997; Tavernier et al., 1996).

In the hypothalamic-pituitary-thyroid (HPT) axis, thyrotropin releasing hormone (TRH) is released from the hypothalamus and acts on the anterior pituitary. As a result, TSH is released, and binds to TSHR on thyrocytes (Boelen et al., 2012). This binding regulates development and growth of the thyroid gland, and stimulates thyroid hormone production:

thyroxine (T4) and tri-iodothyronine (T3). T4 is deiodinated to T3, which acts on many cell types in the body, increasing basal metabolic rate. T3 and T4 act in a negative feedback loop to both the hypothalamus and the pituitary to regulate thyroid hormone levels within the body (Boelen et al., 2012). In addition to being expressed by thyrocytes, TSHR expression has been documented in human adipocytes and has been implicated in lipolysis in both physiological and pathophysiological states (Gagnon et al., 2010; Marcus et al., 1988).

TSH signals through TSHR by activating a cAMP mediated signal cascade, similar to that seen with β-AR. Binding of TSH occurs through the extracellular N-terminal, leucine-rich domain of the receptor, which induces a conformational change through the transmembrane domain and initiates G-protein activation (Davies et al., 2002). In humans, TSH is responsible for modulating the majority of lipolytic signaling in neonates, while effects of catecholamines are insignificant at this particular time, and possibly even inhibitory via α-adrenergic receptors (α–AR) (Marcus et al., 1988). The lipolytic signaling can be observed through *ex vivo* adipocyte stimulation with TSH, and can be inhibited by TSHR-blocking antibodies (Janson et al., 1998).

Signaling through Gi-coupled GPCRs is important for anti-lipolytic signaling in adipocytes. Catecholamines, in addition to Gs-mediated actions, can stimulate α_2-AR; this signaling is dependent on receptor affinity and expression (Lafontan and Berlan, 1995). The most well understood anti-lipolytic effects have been described through neuropeptide Y receptor 1 (NPYR1), A_1-adenosine receptor and EP-3 prostaglandin E_2R (Cai et al., 2008; Liu et al., 2009; Richelsen, 1988; Taggart et al., 2005). In general, stimulation through these receptors activates Gi and inhibits lipolysis by blocking AC activity. Due to the downstream inhibition of lipolysis, these receptors have been described as targets for anti-hyperlipidemic

drugs to reduce excess NEFA release and circulating lipids, which may lead to other metabolic problems, as discussed (Wang and Fotsch, 2006).

1.2.2 Natriuretic peptide receptors in stimulation of lipolysis

In addition to GPCR signaling hormones, natriuretic peptides are potent stimulators of human adipocyte lipolysis. Atrial natriuretic peptide (ANP) and brain natriuretic peptide (BNP) can stimulate lipolysis to a similar extent as isoproterenol, while c-type natriuretic peptides show weaker effects (Sengenes et al., 2000). Human adipocytes express natriuretic peptide receptor (NPR) type A and C, which initiate a signal cascade via the guanylyl cyclase (GC) system (cGMP activation of protein kinase G; PKG), which results in similar lipolytic processing as in the AC system (Sengenes et al., 2003; Stralfors and Belfrage, 1985).

1.2.3 Tyrosine kinase receptors in inhibition of lipolysis

Signaling via tyrosine kinase receptors (TKR) show potent and important anti-lipolytic effects. The insulin receptor, and to a lesser insulin-like growth factor-1 receptor (IGF-1R) are both TKRs expressed by adipocytes, which stimulate glucose uptake and control cAMP levels (Bolinder et al., 1987; Saltiel and Pessin, 2002). These receptors possess an extracellular binding domain, a transmembrane domain and a large intracellular catalytic domain. Stimulation via the insulin receptor initiates a signal cascade of phosphorylation events resulting in the activation of PDE-3B. PDE-3B mediates the degradation of cAMP to 5'-AMP, thus inactivating protein kinase A (PKA) to inhibit lipolysis (Choi et al., 2006).

1.2.4 PKA mediated cellular signaling in GPCR-stimulated lipolysis

Upon stimulation of a GPCR, the α-subunit of the Gs-protein dissociates from its respective β and γ subunits activating downstream pathway-specific targets, depending on the Gα activated (Lagerstrom and Schioth, 2008). In adipocytes two pathways exist. Signaling through the Gαs protein activates AC and PKA, as described (Lafontan and Langin, 2009). Alternatively, signaling through Gαq protein activates phospholipase C (PLC), which cleaves phosphatidylinositol 4,5-bisphosphate (PIP2) to diacylglycerol (DG) and inositol triphosphate (IP3). DG, in turn, activates conventional isoforms of protein kinase C (cPKC) (Carmen and Victor, 2006). The activity of both these kinases, PKA and cPKC, has been implicated in lipolysis.

High cAMP levels in the cell, via GPCR or TSHR stimulation, activates PKA. Four molecules of cAMP bind the two regulatory subunits of PKA (PKAR), inducing a conformational change, which results in the release and activation of the two PKA catalytic subunits (PKAC). To achieve optimal kinase activity, PKAC must be Ser/Thr phosphorylated on its activation loop. PKAC has many phosphorylation targets within the cell, and recognizes the following sequence R-R-X-S/T-Y (Kemp et al., 1977). PKA activity is reduced when PDE-3B is activated, as it degrades cAMP, thereby allowing the PKAR to re-attach to PKAC (Taylor et al., 1990). The two key kinase targets of PKA for lipolytic signaling are perilipin and hormone-sensitive lipase (HSL).

Since PKA regulates many processes within a given cell type, localization allows for specificity with respect to downstream substrates. A-kinase anchoring proteins (AKAPs) bind PKAR via an amphipathic helix domain and localize enzyme activity to specific compartments within the cell (plasma membrane, mitochondria, nucleus etc…) (Pidoux and Tasken, 2010). These AKAPs may also act as scaffolds for substrates and regulatory

molecules, including PDEs and phosphatases, as well as phosphorylation targets (Welch et al., 2010). AKAPs differ in structure, yet share similar functions. To date nearly 50 AKAPs targeting PKAR have been identified (Welch et al., 2010). Recently, PRAJA2, the focus of this thesis, was identified as a novel AKAP and E3 ubiquitin ligase, regulating PKA localization and activity in long-term memory storage in neuroblastoma cells, amongst other kinase-mediated pathways (Lignitto et al., 2011).

1.2.5 Lipid hydrolysis and lipase regulation in lipolysis

Perilipin is a protective coat protein found on the surface of lipid droplets within adipocytes and regulates the storage and utilization of cellular lipids. Perilipin A and B were the earliest identified proteins of the PAT family (perilipin, adipophilin and tail-interaction protein family) implicated in intracellular lipid metabolism (Brasaemle, 2007). These two proteins arise from separate splicing events of the PLIN gene, with perilipin A being the predominant form in mature adipocytes (Greenberg et al., 1993). Perilipin A contains three hydrophobic regions (H1, H2 and H3), important for targeting and anchoring the protein, and an acidic region (Subramanian et al., 2004). Perilipin is one of the most phosphorylated proteins in adipocytes, with 6 serine residues identified as PKA target sites in mouse, Ser492 being essential for lipolysis (Brasaemle et al., 2009). Phosphorylation by the cGMP/PKG cascade has been proposed, but details have not been described (Sengenes et al., 2003). When phosphorylated, perilipin undergoes conformational changes exposing lipids to a series of lipases. This phosphorylation is essential for the activation of HSL (Lafontan and Langin, 2009).

Lipases hydrolyze lipids and are essential in digestion, transport and processing of dietary and stored fats. It is the combined actions of adipose triglyceride lipase (ATGL),

HSL and monoglyceride lipase (MGL), which release the 3 fatty acids from the glycerol backbone of TGs within adipocytes. The catalytic activities of these lipases break the ester bonds joining the fatty acid to the glycerol molecule. This occurs via catalytic residues of the active site located in the α/β hydrolase fold of the enzyme (Watt and Spriet, 2010). The resulting NEFA are shuttled out of the cell and into the bloodstream by fatty acid binding protein-4 (FABP4), while glycerol escapes through an aquaporin channel (Kishida et al., 2000; Matarese and Bernlohr, 1988).

ATGL is a 486 a.a. protein with a molecular weight of 54kDa, which releases a NEFA from a TG, creating a DG, within the lipid droplet of adipocytes. The hydrophobic region of this protein (a.a. 351-360) mediates lipid droplet binding and the protein contains two phosphorylation sites near the C-terminus. These phosphorylation sites Ser^{404} and Ser^{428} are targets of PKA and are important for enzyme activity under stimulated conditions *in vivo* (Pagnon et al., 2012; Zechner et al., 2009). Overexpression of ATGL in mouse differentiated adipocytes increases basal and hormone stimulated lipolysis, while its knockdown decreases NEFA and glycerol release from the cell (Kershaw et al., 2006). Null-mice have blunted lipolysis, more TG accumulation, and achieve a rapid onset of obesity (Haemmerle et al., 2006). Lipolytic action of ATGL is dependent on the catalytic dyad Ser47-Asp166 and activator α/β hydrolase domain-containing protein 5 (ABHD5). Upon stimulation, ABHD5 translocates from the lipid droplet to the cytosol to activate ATGL for TG hydrolysis (Lass et al., 2006; Zechner et al., 2009).

HSL exists in several isoforms with different tissue-dependent promoters (Kraemer and Shen, 2002). Upon phosphorylation by PKA, HSL undergoes a conformational change important for its translocation from the cytosol to the lipid droplet. Once at the lipid droplet, phosphorylated HSL interacts with phosphorylated perilipin and neutral lipids. The C-

terminal domain containing the catalytic triad Ser424-Asp693-His723, is responsible for its enzymatic activity on TG and DG, the latter occurring at a 10-fold higher affinity; this results in a monoglyceride molecule (MG) (Holm, 2003). HSL shows preference for catalysis at the sn-1 and sn-2 positions of the lipid molecule and is reliant on phosphorylation at two PKA-target sites, which were initially characterized in rats (Anthonsen et al., 1998; Raclot et al., 1997).

Once processed to the MG state, the ester bond between glycerol and the final fatty acid can be processed by MGL. MGL is a 302 a.a. protein with a molecular weight of 33kDa (Fredrikson et al., 1986). This enzyme hydrolyzes sn-1(3) and sn-2 ester bonds at equal rates via its catalytic triad Ser122-Asp239-His269 and is not rate limiting in the lipolytic process (Karlsson et al., 1997). After this final round of ester bond hydrolysis, the glycerol backbone and final NEFA are shuttled out of the cell.

An important aspect of lipid metabolism and the lipolytic process in adipocytes is NEFA and glycerol transport. As stated, FABP4 is a lipid binding molecular chaperone, which facilitates shuttling NEFA out of the cell (Matarese and Bernlohr, 1988). Adoption of a β-barrel structure creates a water-filled cavity for non-covalent ligand binding of a single fatty acid (LaLonde et al., 1994). The remaining glycerol backbone is released from the cell via an aquaporin channel. Aquaporin is translocated to the plasma membrane upon catecholamine stimulation and is negatively regulated by insulin (Hibuse et al., 2006; Kishida et al., 2000).

1.2.6 Dysregulation of lipolysis in disease states

Lipolytic activity is tightly regulated in response to feeding, fasting and physical exercise via changes in hormone levels (catecholamines and insulin). This regulation alters

the expression and activity of lipases within the lipolytic pathway (Horowitz and Klein, 2000; Stich et al., 1999). As individuals age, their ability to mobilize fatty acids for fuel becomes diminished. A similar impairment is seen in those who are subjected to chronic stress when β-ARs become desensitized (Blaak, 2000; Coppack et al., 1994). Problems in lipolytic regulation also occur with obesity-associated insulin resistance and subclinical hypothyroidism (SCH), as explained below.

Obesity may develop from a combination of genetic predisposition and environmental factors (Suganami et al., 2012). Fundamentally, obesity is a result of a positive energy imbalance, such that energy intake exceeds energy expenditure. This imbalance often evolves from intake of energy-dense, nutrient poor foods high in fats and sugars combined with a decrease in energy expenditure in today's sedentary lifestyle. Over time, this calorie surplus results in increased TG storage in AT (Sun et al., 2011).

Many obese individuals show comorbidities of insulin resistance. Insulin plays an important inhibitory role in the lipolytic process. Subjects exhibiting insulin resistance will also exhibit problems in turning off the lipolytic process in adipocytes (Reynisdottir et al., 1994). Overall, obese subjects present with increases in plasma NEFA levels, due to their general increased fat mass and disturbed insulin signaling (Arner, 1988). This dyslipidemia results in ectopically deposited lipids in muscle and liver. Often during excess NEFA processing, there is a buildup of harmful byproducts, which is correlated to dysfunction in these tissues (Reynisdottir et al., 1994).

Adipocytes express TSHR and are targets of extra-thyroidal TSH action, resulting in lipolysis (Gagnon et al., 2010; Marcus et al., 1988; Sorisky et al., 2000; Thrush et al., 2012). In SCH in the adult, TSH may influence lipolysis. SCH is characterized by compensatory high levels of circulating TSH (>5mU/L), to maintain normal thyroid hormone levels, in the

presence of mild thyroid failure (Surks and Ocampo, 1996). Studies have shown increases in plasma NEFA and glycerol in SCH patients compared to controls (Caraccio et al., 2005). TSH stimulation of adipocytes *in vitro* leads to induction of mRNA expression and release of IL-6 (Antunes et al., 2008). SCH is associated with insulin resistance and CVD (Maratou et al., 2009; Rodondi et al., 2010; Sorisky et al., 2008).

1.3 A potential link between lipolysis and the ubiquitin-proteasome system

The ubiquitin-proteasome system (UPS) functions to selectively tag and degrade unneeded and damaged proteins within the cell, via protease activity. Ubiquitin (Ub) is a 76 a.a. peptide molecule, which, when linked to a protein via a lysine residue, acts as a signal for proteasomal degradation (Wilkinson, 2005). Ubiquitination is a three-step process; firstly, ubiquitin-activating enzyme (E1) hydrolyzes ATP and adenylates ubiquitin (Ciechanover et al., 1982). Next, the ubiquitin molecule is transferred to a cysteine residue in the E1 active site and a second adenylation occurs. Subsequently, ubiquitin is transferred to ubiquitin-conjugating enzyme (E2), which proceeds to complex with ubiquitin ligase enzyme (E3) within the cell. E3 ligases recognize target proteins within the cell and act as a scaffold to transfer ubiquitin from E2 to the substrate protein (Ardley and Robinson, 2005). This mechanism may be used in maintenance of enzyme functions through processing of regulatory units (including PKA), and may be linked to various disease states (Chain et al., 1999).

1.4 PRAJA2: A novel AKAP and E3 ubiquitin ligase

PRAJA2 is a homolog of rat protein neurodap1 (NDAP1; expressed in neurons) and has 52% sequence similarity to PRAJA1, an E3 ubiquitin ligase expressed in the brain associated with x-linked mental retardation (Mishra et al., 1997). The *pja2* gene is 75,286bp

in length and is located on chromosome 5 at cytogenic band q21.3 in humans. Translation of *pja2* results in a 708 amino acid product with a molecular weight of ~78kDa. The mature protein contains an R-binding domain (a.a. 531-631) and a RING-H2 domain (a.a. 631-708). The former binds PKAR via an α-helix, while the latter contains intrinsic E3-ubiquitin ligase activity (Lignitto et al., 2011).

1.4.1 Control of PKA stability and signaling by the RING ligase PRAJA2

In 2011, Lignitto *et al.* characterized PRAJA2 as a novel E3 ubiquitin ligase that acts on PKAR. Lignitto *et al.* (2011) showed, in neurons, that PRAJA2 forms a stable complex with PKAR, localizing PKA to the plasma membrane, perinuclear region and cellular organelles in an AKAP-like manner (Lignitto et al., 2011). Upon cellular stimulation with isoproterenol or forskolin, cAMP binds PKAR allowing for PRAJA2 phosphorylation at residues Ser342 and Thr389 by PKAC. This phosphorylation promotes PRAJA2-mediated ubiquitination and subsequent proteosomal degradation of PKAR, thereby prolonging activity of PKAC and sustaining substrate phosphorylation level within the cell (Figure 1) (Lignitto et al., 2011). Further experiments show the significance of this cellular action on PKA-mediated cAMP response element-binding protein (CREB) phosphorylation, up-regulation of *c-fos* transcription and the ultimate impact on long-term memory pathways in hippocampal neurons.

1.4.2 Expression of PRAJA2 in thyroid cancer

In 2012, Cantara *et al.* investigated the expression of PRAJA2 in thyroid cancer samples. Binding of TSH to TSHR in differentiated thyroid cancer cells stimulates growth and cancer progression via cAMP/PKA pathways (Schweppe et al., 2009; Zielke et al., 1999). Levels of PRAJA2 were quantified in differentiated papillary thyroid cancer (PTC),

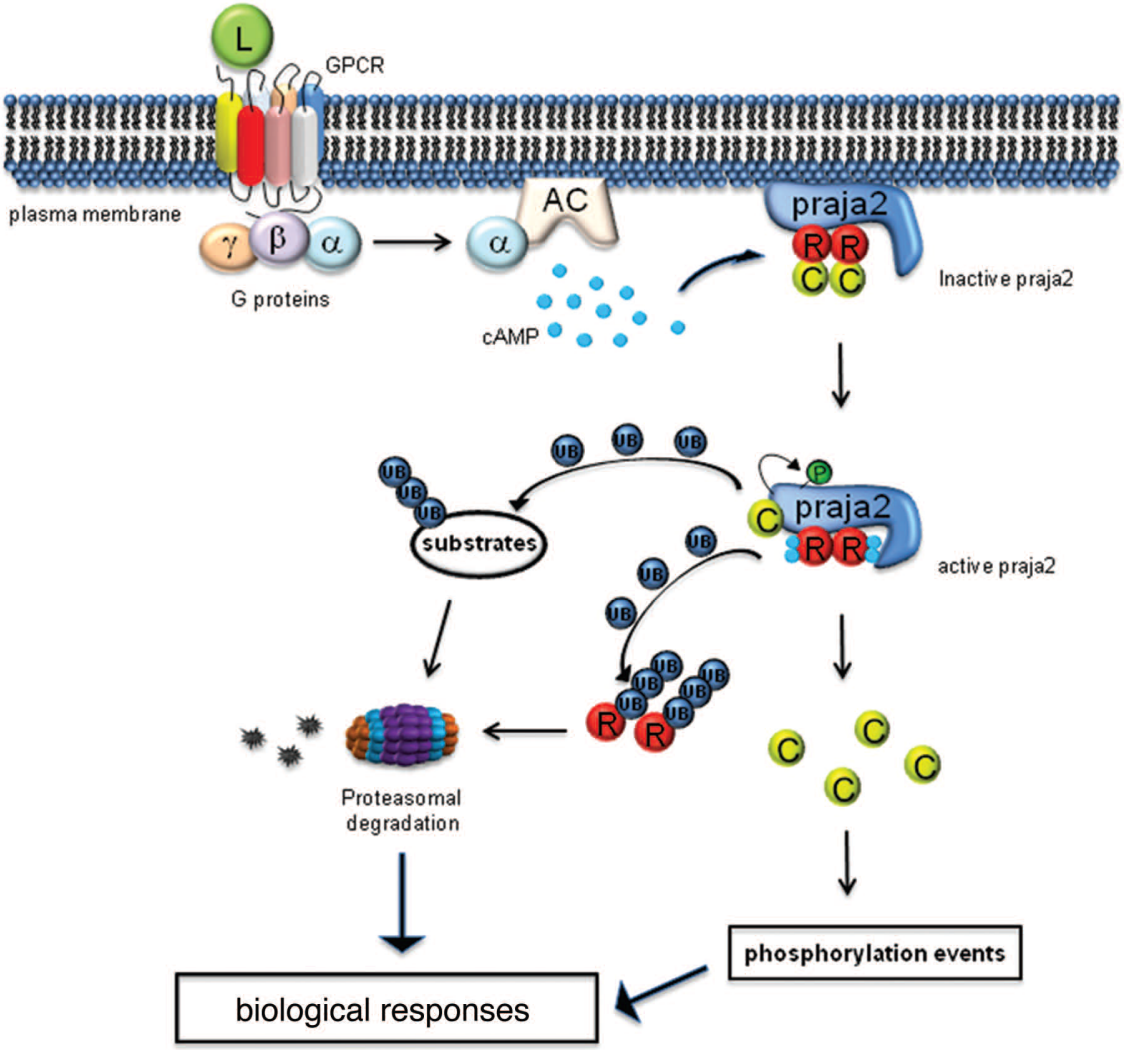
L
GPCR
plasma membrane
γ
β
α
G proteins
α
AC
cAMP
praja2
R R
C C
Inactive praja2
UB
substrates
P
praja2
active praja2
Proteasomal
degradation
phosphorylation events
biological responses

Figure 1. ***Proposed role of PRAJA2 in PKA signaling.*** Ligand (L) binding to its G-protein coupled receptor (GPCR) at the plasma membrane stimulates adeylate cyclase (AC) and elevates intracellular cAMP levels. cAMP binding to R subunits of PKA holoenzyme releases the catalytic moiety of PKA (C), which in turn phosphorylates PRAJA2. Phosphorylated PRAJA2 ubiquitinylates and degrades R subunits through the proteasome pathway. Accumulation of free active PKAC (C) sustains substrate phosphorylation, positively impacting of the rate and magnitude of cAMP signaling. Proteolysis of other PRAJA2 substrates may also contribute to the hormone responses. **Figure taken from:** (Lignitto et al., 2011).

anaplastic thyroid cancer (ATC), benign nodules (BN) and normal tissue (NT) (Cantara et al., 2012). PRAJA2 was more highly expressed in PTC, at the mRNA and protein level, when compared to levels in ATC, BN and NT (Cantara et al., 2012). PRAJA2 mRNA expression showed inverse correlation to the aggressive potential of the tumor within the PTC subtype for both cell-line and tissue samples (Cantara et al., 2012). This study suggested that PRAJA2 may be a novel cancer-related gene expressed in TSH-responsive cells that is linked to tumor histotype.

1.4.3 Proteolysis of MOB1 by PRAJA2 attenuates Hippo signaling and supports glioblastoma growth

In 2013, Lignitto *et al.* examined PRAJA2's role in glioblastoma growth and tumor survival via the HIPPO pathway. Mps one binder 1 (MOB1) was identified as a direct target for PRAJA2 E3 ligase activity (Lignitto et al., 2013). Briefly, MOB1 positively regulates kinase activity of large tumor suppressor (LATS1/2) leading to the phosphorylation, and nuclear exclusion, of the yes-associated protein 1 (YAP) transcription factor (Hergovich, 2011). When PRAJA2 is active, MOB1 is ubiquitinated and degraded by the proteasome. This inactivates LATS1/2 kinase activity and allows YAP to translocate into the nucleus, leading to transcription of genes involved in cell proliferation and tumor growth. Lignitto *et al.* showed PRAJA2 expression at the mRNA and protein levels to be 2-3 folds higher in clinical high-grade glioblastoma tumors when compared to lower-grade astrocytomas, supporting its involvement in attenuating HIPPO suppression and sustaining tumor growth (Lignitto et al., 2013).

1.4.4 Differential PKA activation and AKAP association determines cell fate in cancer cells

Hedrick *et al.* showed colorectal cancer cells (CRC) utilize various AKAPs to regulate cell fate. Upon stimulation via transforming growth factor beta (TGFβ), Smad3 binds PKAR, releasing and activating PKAC in a cAMP-independent manner. In this context, PKA localization and kinase activity is mediated by AKAP149, causing disruption of survivin and XIAP phosphorylation, allowing for their interaction (Chowdhury et al., 2011). This complex ultimately relieves caspase3/7 inhibition promoting apoptosis and cell death. Alternatively, upon cAMP-dependent activation of PKA via growth factor stimulation of the IGF1R, PRAJA2 becomes the main effector AKAP (Hedrick et al., 2013). Phosphorylation of survivin and XIAP proteins disrupts their interactions with each other. This stabilization of XIAP increases its inhibitory action on caspase3/7, resulting in a pro-survival cell fate (Hedrick et al., 2013). These results correlate with previous studies suggesting PRAJA2 as a pro-survival/growth oncogene as shown in thyroid cancer and glioblastomas (Cantara et al., 2012; Lignitto et al., 2013).

1.4.5 Role of the SIK2-p35-PRAJA2 complex in pancreatic β-cell functional compensation

In 2014, Sakamaki *et al.* detailed the role of PRAJA2 in mediating glucose stimulated insulin secretion (GSIS) in β-cells of the pancreas. Under basal conditions cyclin-dependent kinase 5 (CDK5) is bound to its regulatory subunit (activator; CDK5R1) and is able to phosphorylate voltage dependent calcium channels (VDCC) suppressing calcium influx and restraining insulin secretion (Wei et al., 2005). Upon glucose stimulation, salt-inducible kinase 2 (SIK2; AMPK related kinase) is stabilized, leading to the phosphorylation of CDK5R1 and promotion of its degradation via PRAJA2-mediated ubiquitinylation

(Sakamaki et al., 2014). This blunts CDK5 kinase activity, relieving VDCC phosphorylation, increasing calcium ion influx and promoting insulin secretion. This study shows the importance of SIK2-CDK5-PRAJA2 complex in glucose homeostasis via GSIS regulation (Sakamaki et al., 2014). Additionally, it suggests activation of SIK2 and PRAJA2 in the β-cell may prove beneficial for treating individuals with insulin secretory deficits in the context of T2D.

1.5 Model system

In vitro models are invaluable for studying effects of metabolism, proliferation, differentiation and survival of adipocytes. In this thesis, a human primary differentiated adipocyte model is used. Primary human preadipocytes can be isolated and cultured from the SVF of various AT depots in the body. These isolated cells can then be cultured and matured into adipocytes upon induction of differentiation (adipogenesis). Adipogenesis is induced by supplementing growth medium with 3-isobutyl-1-methylxanthine (IBMX; 0.25mM), insulin (850nM), indomethacin (100μM) and dexamethasone (0.5μM) (Gagnon et al., 2013). These factors stimulate CCAAT-enhancer binding proteins (C/EBP transcription factors), as well as, other fatty acid storage and glucose metabolism regulators such as PPARγ (Garten et al., 2012; Park et al., 2012; Rosen et al., 2002; Wu et al., 1999). This protocol typically results in ~60-70% differentiation (Hauner et al., 2001).

Insulin acts through IGF1R and the insulin receptor throughout the differentiation process promoting glucose uptake and *de novo* lipogenesis for lipid storage. IBMX inhibits phosphodiesterase activity, amplifying cAMP levels and PKA activity within the cell (Gregoire, 2001; Cristancho and Lazar, 2011). PKA contributes to differentiation by phosphorylating and therefore activating CREB and subsequently C/EBPβ. Additionally,

stimulation of the glucocorticoid receptor by dexamethasone increases expression of C/EBPδ and acetylation/binding of C/EBPβ to adipogenic genes (Gregoire, 2001; Cristancho and Lazar, 2011). Indomethacin acts as a PPARγ agonist, similar to thiazolidinediones, increasing C/EBPα creating a positive feedback loop with PPARγ and contributing to promotion of lipid storage. C/EBPβ and δ are transiently induced during the early stages of adipocyte differentiation, while C/EBPα is up-regulated during the terminal stages of adipogenesis (Gregoire, 2001; Cristancho and Lazar, 2011).

Limitations of this model include donor availability, cell passage number, variable differentiation and donor differences (BMI, age, sex etc…). In culture, preadipocytes lose their ability to differentiate after 3-4 passages. Specifically this human differentiated model results in a mixed population of precursor and differentiated cell types, which at times may confound results. The adipocyte precursors of the stromal vascular population differ from mesenchymal and hematopoietic stem cells and are documented as $CD14^{-}/CD34^{+}/Cd31^{-}$ (Sengenes et al., 2005). Due to its source, the human model is relevant and representative. Specifically, with respect to this thesis, a human model is essential to avoid potential species-specific differences in the molecular regulation of lipolysis by TSH.

An established and widely used non-human cellular model, in this field, is the murine 3T3-L1 preadipocyte line. These immortalized cells were first isolated from Swiss 3T3 mouse embryonic tissue and have a fibroblastic appearance (Green and Meuth, 1974). This cell line can be passaged many more times than human preadipocytes in culture and under proper conditions can be induced to differentiate into cells that appear similar to adipocytes, both morphologically and in their ability to respond as energy balancing endocrine cells (Gregoire, 2001; Cristancho and Lazar, 2011). Although widely used, this line has a number

of pitfalls including its embryonic stage, aneuploid nature, murine origin, lack of depot specificity and species of origin (Cornelius et al., 1994).

1.6 Rationale

PRAJA2 has been suggested to function as both an AKAP and an E3 ubiquitin ligase. Lignitto *et al.,* 2011 identified PKA as the first known target of PRAJA2 action. It was shown to anchor PKA to the cellular membrane (AKAP) and facilitate the proteasomal degradation of PKA regulatory subunits upon cellular stimulation with forskolin or isoproterenol. Additionally, Cantara *et al.,* 2012 showed increased abundance of PRAJA2 in TSH-responsive thyroid cancer cells, PTC, compared to ATC, suggesting PRAJA2 may have a role in TSH-stimulated cellular processes. Since adipocytes in WAT express functional TSHR and the lipolytic pathway in these cells is PKA-dependent, the regulation of lipolysis by TSH and isoproterenol may involve PRAJA2.

1.7 Hypothesis

It was hypothesized that PRAJA2, if present in adipocytes, would regulate the lipolytic response stimulated by TSH or isoproterenol. It was proposed that PRAJA2 would be phosphorylated in a PKA-dependent manner while co-localizing with PKAR. Additionally, the down-regulation of PRAJA2 would reduce lipolytic signaling via PKA through limiting its E3 ligase action on PKAR.

1.8 Objectives

The purpose of this project was to assess the role of PRAJA2 in TSH- and isoproterenol-stimulated lipolysis. These studies involved the use of primary human

adipocytes, differentiated from preadipocytes, which were isolated from the subcutaneous depot of patients undergoing elective abdominal surgery.

Objective 1: Characterize the expression of PRAJA2 in primary human differentiated adipocytes.

Objective 2: Investigate protein modifications and proteins interacting with PRAJA2 in primary human differentiated adipocytes, which may elucidate the mechanism through which PRAJA2 regulates the lipolytic pathway.

Objective 3: Determine the effect of down-regulating PRAJA2 expression on TSH- and isoproterenol-stimulated lipolysis in primary human differentiated adipocytes.

2. MATERIALS AND METHODS

2.1 Isolation of human abdominal subcutaneous stromal preadipocytes

Abdominal subcutaneous adipose tissue was obtained from 12 weight-stable female patients undergoing elective abdominal surgery (approved by the Ottawa Health Science Network Research Ethics Board). The age of the patients studied was 49 ± 11 years and the body mass index was 32.3 ± 10.4 kg/m^2 (mean ± S.D.), neither parameter showed a correlative effect on results presented. Adipose tissue was removed, and dissected to rid it of fibrous connective tissue and blood vessels. Subsequently, the tissue was digested with collagenase CLS type I (600 U/g tissue; Worthington Biochemical Corporation, Lakewood, NJ, USA) for 1 hour at 37^{o}C on nutator shaker. After digestion, the tissue was subjected to size filtration through sterile 200 μm nylon filter to remove any remaining connective tissue and debris. The filtrated sample was then centrifuged (200 xg; 20 min) to remove floating mature adipocytes. After centrifugation, sample was subject to progressive size filtration, through sterile 100 μm, 50 μm and 25 μm nylon filters, and centrifuged a second time (200 xg; 20 min) to ensure elimination of any remaining connective tissue, debris, or mature adipocytes from the sample. The remaining pellet was treated with red blood cell lysis buffer (155 mM NH_4Cl, 5.7 mM K_2HPO_4, 0.1 mM EDTA; pH 7.3) for 5 minutes, after which Dulbecco's Modified Eagle Medium (DMEM) supplemented with 10% fetal bovine serum (FBS), antibiotics (100 U/mL penicillin, 0.1 mg/mL streptomycin; Life Technologies Inc., Burlington, ON, Canada) and antifungal agents (75 U/mL nystatin; Calbiochem, Etobicoke, ON, CA) were added; designated growth medium. Cells were either plated (5-10x10^3 cells/cm^2) and grown for cryopreservation until use, or directly passaged and expanded before being subjected to differentiation. Alternatively, for some experiments, commercially

acquired human preadipocytes from Zen-Bio; North Carolina, NC, USA were used (Gagnon et al., 2013)

2.2 Culture and differentiation of human subcutaneous preadipocytes

Subcutaneous stromal preadipocytes were maintained in growth medium, with changes every two days. Each passage was performed with the addition of 1X TrypLE (Life Technologies Inc., Burlington, ON, Canada). Cells were enumerated using a Neubauer hemocytometer and seeded at a density of $2.5x10^4$ cells/cm^2 in growth medium. The following day, the seeded cells were placed in fresh growth medium supplemented with the following adipogenic inducers: 850 nM insulin (Roche, Laval, QC, Canada); 0.5 μM dexamethasone (Steraloids, Newport, RI, USA); 0.25 mM isobutylmethylxanthine; and 100 μM indomethacin (both from Sigma-Aldrich, St. Louis, MO, USA); designated adipocyte differentiation medium, for 2 weeks. For some experiments differentiating cells received partial media changes, equal to half of the initial volume of adipocyte differentiation medium, every 3-4 days throughout the two-week process. After the two-week induction, cells were rinsed and placed back in growth media for 2-3 days before experimental treatment. Differentiated adipocytes were photographed with Nikon Coolpix 995 digital camera mounted on Nikon Eclipse TS-100 microscope at magnifications between 100X and 400X. Typically 60-70% differentiation was achieved (Gagnon et al., 2013).

2.3 Stimulation of differentiated human adipocytes with TSH or isoproterenol

After two days in growth medium, human differentiated adipocytes were stimulated as follows. Adipocytes were first rinsed with 1mL of filter-sterilized assay buffer (DMEM + 4% fatty acid-free BSA; Roche, Laval, QC, Canada, 100 U/mL penicillin, 0.1 mg/mL streptomycin). Cells were then stimulated with 5 mU/mL bovine TSH (bTSH), 50 mU/mL

bTSH, 1 μM isoproterenol or vehicle (water) (both from Sigma-Aldrich, St. Louis, MO, USA). Treatments were removed after the indicated stimulation period and processed for lipolysis, mRNA expression, immunoblot, immunoprecipitation, or immunohistochemistry analysis.

2.4 RNA isolation and DNaseI treatment

After stimulation, the medium was removed and 1 mL Qiazol reagent (Qiagen, Venlo, Limburg, Netherlands) was added to the cells for 5 minutes at room temperature. Samples were scraped, transferred to 1.5 mL microfuge tubes, and flash-frozen in liquid nitrogen for storage at -80^{o}C. Qiazol-treated samples were thawed at room temperature. After thawing, 200 μL of chloroform was added, and samples were mixed by inversion for 3 minutes. After mixing, samples were centrifuged (10,000 xg, 10 min, 4^{o}C) and the upper aqueous layer was transferred to a new tube. Subsequently, 500 μL of isopropanol was added to the aqueous layer, samples were mixed by inversion, and left to incubate for 10 minutes at room temperature. Following incubation, samples were centrifuged (10,000 xg, 10 min, 4^{o}C), the supernatants discarded and the pellets were re-suspended in 1 mL 75% ethanol (EtOH; in DEPC treated water). Centrifugation was repeated (7,500 xg, 5 min, 4^{o}C) after which the supernatants were discarded and the pellets were air-dried. Dried pellets were then re-suspended in 50 μL DEPC-treated water, incubated at 65^{o}C for 10 minutes and placed on ice.

These RNA isolates were subsequently subjected to DNaseI treatment to remove any contaminating DNA from the samples, using DNA Treatment & Removal kit (Life Technologies Inc., Burlington, ON, Canada). Following the manufacturer's protocol, 5 μL 10X DNaseI buffer and 1 μL rDNaseI were added to each sample and samples were incubated at 37^{o}C for 30 minutes. Next, 5 μL of DNaseI inactivation buffer was added to

each sample and samples were subjected to mixing by inversion for 2 minutes. Finally, samples were centrifuged (10,000 xg, 10 min, 4^{o}C), after which supernatants were transferred to new 1.5 mL microfuge tubes and stored at -80^{o}C until quantification.

2.5 RNA quantification and quality analysis

RNA was quantified using Quant-it Ribogreen RNA assay kit (Life Technologies Inc., Burlington, ON, Canada), with 16S/23S rRNA as a standard. Isolates were thawed at room temperature and diluted (25-100X) in 1X Tris-EDTA (TE) buffer. Samples were assayed in triplicate; 1 µL of diluted RNA was added to 99 µL TE buffer in a black-bottom 96-well plate. Subsequently, 100 µL of Ribogreen reagent was added to each well. Fluorescence readings were taken (excitation: 485 nm, emission: 520 nm) using FLUOstar Galaxy spectrophotometer (BMG Labtech, Ortenberg, Germany). For quality assessment 1 µg of RNA sample was run on 1% denaturing formaldehyde agarose gel to confirm samples had not degraded. Ethidium Bromide was used as a visualizing agent and gels were imaged on ChemiDoc-It TS2 Imaging System (Ultra-Violet Products Ltd., Upland, CA, USA)

2.6 Reverse Transcription and qPCR

Samples of 0.5-2.5 µg RNA were brought to a volume of 25 µL with nuclease-free water. Subsequently, 5 µL of 0.5 µg/µL random primers (Life Technologies Inc., Burlington, ON, Canada) were added and samples were incubated at 85^{o}C for 3 minutes; followed by incubation on ice. After cooling, 12 µL of sample were added to 8 µL reverse transcription mix (1.25 mM dNTP, 1.4 U/µL RNase OUT, 12.5 U/µL MMLV-RT, in 1X RT buffer; all from Life Technologies Inc., Burlington, ON, Canada) or negative control mix (no MMLV-RT) and samples were incubated at 43^{o}C for 1 hour. Following the incubation, MMLV-RT

was inactivated by heating samples to 92^{o}C for 10 minutes. The newly synthesized cDNA samples were stored at -20^{o}C until use for qPCR.

Sample mRNA expression levels were analyzed via qPCR. Sample cDNA (2 µL) was added to primers (f.c. 100 nM) and THUNDERBIRD SYBR qPCR Mix (TOYOBO, Osaka, OSK, Japan), to give a total reaction volume of 20 µl. PCR reactions were then performed using Light Cycler Carousel (Roche, Laval, QC, Canada). Conditions were set to the following parameters: 10 minutes at 95°C, followed by 45 cycles each of 15 seconds at 95°C and 1 minute at 60°C. The primers used for PCR analyses were as follows: PRAJA2, forward, 5'-GGTTACAGTACAATGAAGTC -3' and reverse, 5'-CAACTCCTAGTCCATCTG-3'; SREBP-1c forward, 5'-GACCGACATCGAAGACATGC-3' and reverse, 5'-GGCATGGACGGGTACATCTT-3'. Samples were diluted 1000X for analysis of 18S rRNA as an internal control. Diluted cDNA (2 µL) was added to 18S pre-developed TaqMan probe and TaqMan qPCR mix (Life Technologies Inc., Burlington, ON, Canada), to give a total reaction volume of 20 µl. Conditions were set to the following parameters: 10 min at 95°C, followed by 45 cycles each of 15 sec at 95°C and 1 min at 60°C.

2.7 Lowry protein assay

Following stimulation, cells were rinsed with 1 mL PBS and solubilized in Laemmli buffer (2% SDS, 10% glycerol, 60 mM Tris pH 6.8, 0.002% bromophenol blue) (Laemmli, 1970). The resulting cell lysates were scraped, collected using a 26G syringe and boiled for 5 minutes. Protein was quantified via a modified Lowry assay, using Bio-Rad DC protein assay (Bio-Rad, Hercules, CA, USA) with bovine serum albumin (BSA) as a standard. Samples were thawed and assayed in triplicate; 2-5 µL of sample were diluted to a final volume of 200 µL with water. First, 20 µL of deoxycholate (DOC; 1.5 mg/mL) were added;

samples were vortexed and incubated for 10 minutes at room temperature. Next, 20 µL of trichloroacetic acid (TCA; 72% v/v) were added; samples were vortexed and centrifuged (21,000 xg 10 min, room temperature). Following centrifugation, supernatants were discarded and pellets were air-dried for one hour. Pellets were re-suspended in 25 µL Bio-Rad Reagent A' (commercially supplied reagents S and A, 1:50), incubated for 5 minutes and then 200 µL of Bio-Rad Reagent B was added. After a 15 minute incubation, 200 µL of sample was transferred to 96-well microplate and absorbance readings were taken at a wavelength of 750 nm, using FLUOstar Galaxy spectrophotometer.

2.8 Immunoblot analysis

Equal amounts of solubilized protein (5-50 µg), or equal volumes (15-50 µL) for immunoprecipitation samples, were resolved using SDS-PAGE (7.5% to 15% acrylamide). Gel resolution was performed at 200V for 45-60 minutes, and subsequently electrophoretically transferred to a nitrocellulose membrane (Sigma-Aldrich, St. Louis, MO, USA) at 70V for a time period ranging from 1 hour to 1 hour and 45 minutes, depending on the molecular mass of the protein being assessed. Once transferred, membranes were rinsed with 1X PBS and blocked with 5% skim milk in 1X PBS/0.1%Tween20 for 1 hour to prevent non-specific binding of antibodies used for immunoblotting. Membranes were rinsed with 1X PBS and probed overnight at 4^{o}C on Labquake rotator with primary antibodies against the following proteins: PJA2 (1:500-1:2000; Sigma-Aldrich, St. Louis, MO, USA), mitogen-activated protein kinase (MAPK: ERK1/2; 0.25µg/mL; Millipore, Billericia, MA, USA), fatty acid synthase (FAS; 1:1000; BD Biosciences, Mississauga, ON, Canada), phospho-PKA substrate (RRXS*/T*; pPKAsub; 1:1000; Cell Signaling Technology, Beverly, MA, USA), protein kinase B (Akt; 1:1000; Cell Signaling Technology, Beverly,

MA, USA), PKAR2 (1:1000; Abcam, Cambridge, England, UK). After incubation with primary antibody, membranes were washed twice with 1X PBS/0.1%Tween20 for 15 minutes at room temperature. Membranes were subsequently incubated for 1 hour with the appropriate horseradish peroxidase (HRP)-conjugated secondary antibody (anti-rabbit or anti-mouse, 1:500-1:50,0000) diluted in 5% skim milk in 1X PBS. Following incubation, membranes were washed once for 15 minutes and three times for 5 minutes in 1X PBS/0.1%Tween20. Membranes were rinsed 5 times in 1X PBS and subjected to chemiluminescent HRP substrate detection solution (EMD Millipore, Billerica, MA, USA) for 5 minutes. Immunoreactive detection was captured by exposing membranes to film and processing the film using a Feature-SRX-101A developer (Konica Minolta, Chiyoda, Tokyo, Japan). Relative band intensity was quantified and expressed as integrated optical density (IOD) units using AlphaEaseFC software (Alpha Innotec Co., version 4.0.0).

For analysis of protein transfer to the nitrocellulose membrane, membranes were incubated with 0.1% PonceauS in 5% v/v acetic acid (Sigma-Aldrich, St. Louis, MO, USA) for 20 minutes at room temperature on orbital shaker. Following incubation, membranes were rinsed with dH_2O or 1X PBS and visually assessed for disparity in transfer. Additionally, as a loading control for experiments comparing protein expression in preadipocytes versus differentiated adipocytes, Coomassie Brilliant Blue staining was performed. Membranes were incubated in 0.01% Coomassie brilliant blue R-250 (Life Technologies Inc., Burlington, ON, Canada) in a solution of 40% methanol, 10% acetic acid, 50% water for 10 minutes with shaking. Following incubation, membranes were rinsed 3 times and washed 3 times for 10 minutes on orbital shaker in a solution containing 25% isopropanol, 10% acetic acid, 65% water. Membranes were then rinsed 3 times with water or 1X PBS and densitometric analysis was performed. Relative protein content was quantified

between 26-55kDa in each lane and data expressed as integrated optical density (IOD.) units using AlphaEaseFC software (Alpha Innotec Co., version 4.0.0).

2.9 Triglyceride extraction and quantification

Cells were rinsed with 500 μL of PBS and cellular lipids were extracted using isopropanol/heptane (2:3) solution, in a two-step procedure. The cells were first incubated in 0.5mL isopropanol/heptane solution at room temperature for 30 minutes, followed by a second 15-minute incubation. After each incubation, the isopropanol/heptane solution was collected in a glass test tube and dried under N_2 stream using N-EVAP model 112 (Organomation Associates Inc., Manual, NV, USA). Extracts were stored at -20^{o}C until quantification.

Triglycerides were quantified using Triolein as a standard (MP Biomedicals Inc., Santa Ana, CA, USA). Dried lipid extracts were re-suspended in 300 μL of isopropanol. Samples were assayed in triplicate; 10 μL of sample were added to 50 μL isopropanol in a 96-well plate. Subsequently, 30 μL of saponification reagent (18 M KOH in 25% isopropanol) were added and the plate was incubated for 10 minutes at room temperature. Following incubation, 60 μL of 3 mM sodium metaperiodate reagent (3 mM sodium metaperiodate, 100 mM ammonium acetate; in 6% acetic acid) and 60 μL of acetylacetone reagent were added. The plate was then incubated for 15 minutes at 65^{o}C. Samples were left to cool to room temperature and absorbance readings were read at a wavelength of 405 nm, using FLUOstar Galaxy spectrophotometer. TG was expressed as μg/mg protein, as determined by the modified Lowry assay.

2.10 Glycerol quantification

After cellular stimulation, conditioned medium was collected from the cells into chilled 1.5 mL microfuge tubes and centrifuged (500 xg, 5 min, no brake at RT). Following centrifugation, supernatants were transferred to new, chilled microfuge tubes. Glycerol in the medium was quantified according to Zen-Bio protocol (Zen-Bio, North Carolina, NC, USA), with glycerol as a standard (Sigma-Aldrich St. Louis, MO, USA). Samples were assayed in triplicate; 50 µL of sample were added per well in a 96-well plate. To this, 50 µL of glycerol reagent for enzymatic glycerol quantification (Sigma-Aldrich St. Louis, MO, USA) were added and the plate was incubated in darkness at room temperature for 15 minutes. Absorbance readings were taken at a wavelength of 540 nm, using FLUOstar Galaxy spectrophotometer. Glycerol content was expressed as µmol/mg protein, as determined by the modified Lowry assay.

2.11 Non-esterified fatty acid quantification

After cellular stimulation, conditioned medium was collected from the cells into chilled 1.5 mL microfuge tubes and centrifuged (500 xg, 5 min, no brake at RT). Following centrifugation, supernatants were transferred to new, chilled microfuge tubes. NEFA in the conditioned medium was quantified using HR-series NEFA-HR(2) kit (Wako Diagnostics, Richmond, VA, USA), with oleic acid as a standard. Samples were assayed in triplicate; 5 µL of sample were added per well in a 96-well plate. To this, 225 µL of NEFA-HR reagent A were added and the plate was incubated at 37^{o}C for 10 minutes. Subsequently, 75 µL of NEFA-HR reagent B were added and the plate was incubated at 37^{o}C for 10 minutes. Samples were left to cool and absorbance was read at a wavelength of 540 nm, using

FLUOstar Galaxy spectrophotometer. NEFA content was expressed as μmol/mg protein, as determined by the modified Lowry assay.

2.12 Immunoprecipitation

After stimulation, cells were rinsed with 1 mL 1X PBS and incubated on ice for 15 minutes with 0.5 mL lysis buffer (1% NP-40, 200 μM Na_3VO_4, 0.1 mg/ml PMSF, 10 μg/ml aprotinin, 10 μg/ml leupeptin, 4 μg/ml benzamidine, 50 mM NaF, 1 μM β-glycerophosphate, 5 mM NaPPi, in 1X PBS). Samples were harvested via scraping, transferred to 1.5 mL chilled microfuge tubes and mixed thoroughly by pipetting up and down several times. Subsequently, samples were centrifuged (18,000 xg, 10 min, 4^{o}C) and supernatant was transferred to new microfuge tubes avoiding the lipid layer. Three aliquots of 5 μL were used for BCA protein determination and remaining sample was processed for immunoprecipitation as outlined below.

Two 300 μL aliquots of protein A-sepharose beads (Sigma-Aldrich, St. Louis, MO, USA) or protein G-sepharose beads (Life Technologies Inc., Burlington, ON, Canada) were rinsed twice by centrifuging (18,000 xg, 1 min, 4^{o}C) and re-suspending the pellet in 300 μL lysis buffer. In one set of microfuge tubes, 40 μL of washed sepharose beads were combined with the obtained cellular lysate. In a second set of tubes, 40 μL of washed sepharose beads was combined with 460 μL lysis buffer and antibody appropriate for IP (2 μg rabbit anti-PJA2; Sigma-Aldrich, St. Louis, MO, USA; 1:50 (10 μL) rabbit anti-pPKAsub (RRXS*/T*); Cell Signaling Technology, Beverly, MA, USA; 2.5 μg mouse anti-PKAR2; Abcam, Cambridge, England, UK). Both sets of microfuge tubes were incubated for 1 hour at 4^{o}C with rotation on nutator. The protein A/G-sepharose-antibody complex was then centrifuged (18,000 xg, 1 min, 4^{o}C) and rinsed with 0.5 mL lysis buffer. Both sets of microfuge tubes

were then centrifuged (18,000 xg, 1 min, 4°C) and 0.8-1.5 mg of protein from the cleared lysate (as per BCA protein determination assay below) was transferred to the sepharose bead-antibody complex. Additionally, 40 µL of excess cleared lysate was combined with Laemmli buffer, boiled for 5 min and stored at -20°C for immunoblot analysis. Cleared lysates were incubated with protein A/G-sepharose - antibody complex overnight at 4°C with rotation. The following day, incubated samples were centrifuged (18,000 xg, 1 min, 4°C) and bead-antibody-antigen IP complexes were rinsed 5X with 0.5 mL lysis buffer. Upon final centrifugation, IP complexes were re-suspended in 75 µL 1X Laemmli buffer, briefly vortexed, boiled for 5 min and stored at -20°C until immunoblot analysis. Samples were centrifuged (21,000xg, 5 min) prior to loading for SDS-PAGE to pellet the sepharose beads.

2.13 Bicinchoninic acid protein determination

Protein was quantified via BCA assay, using BCA Protein Assay Reagent Kit (Pierce, Rockford, IL, USA) with bovine serum albumin as a standard. Samples were assayed in triplicate. 5 µL of sample was diluted to a final volume of 250 µL with lysis buffer and 250 µL of water was added. Following sample dilution, 0.5 mL BCA reagent cocktail was added to each sample, reagent cocktail consisted of kit reagents MA, MB and MC combined in at a ratio of 50:48:2 v/v/v respectively. Samples were mixed and incubated for 1 hour at 65°C. Subsequently, samples were transferred to cuvettes and left to cool to room temperature. Absorbance readings were taken at a wavelength of 562 nm, using an Ultrospec 3100 pro spectrophotometer (GE Healthcare Life Sciences; Baie d'Urfé, QC, CA).

2.14 DNA vector preparation and analysis

Packaging vectors: psPAX2 (Addgene plasmid 12260) and pMD2.G (Addgene plasmid 12259) (Addgene, Cambridge, MA, USA); pTRIPZ inducible lentiviral non-

silencing control: CTTACTCTCGCCCAAGCGAGAG (ThermoFisher Scientific, Ottawa, ON, CA); pTRIPZ inducible lentiviral human PDGFR-β shRNA: TTTACCACCTCAGTAACTC and three pTRIPZ inducible lentiviral human PJA2 shRNA: TTCAAATATAGGTTCACTG, TGAGGATTGATCTTTTTCT and TGTTGTTTCGTACTAACCA (ThermoFisher Scientific, Ottawa, ON, CA) were used. DNA vectors were prepared using the maxiprep protocol from 500 mL DH5-α *E.* coli overnight cultures grown in Luria Broth (LB; Life Technologies Inc., Burlington, ON, Canada) with 100 μg/mL ampicillin at 37^{o}C with shaking (225 rpm).

First, cultures were centrifuged (6000 xg, 15 min, 4^{o}C). Supernatants were discarded and pellets re-suspended in 10 mL P1 re-suspension buffer (50 mM TrisHCl pH 8.0, 10 mM EDTA, 100 μg/mL RNase A). Subsequently, 10 mL of P2 lysis buffer (200 mM NaOH, 1% w/v SDS) were added, mixed and incubated for 5 minutes at room temperature. After incubation, 10 mL of P3 neutralization buffer (3.0 M potassium acetate, pH 5.5) were added, mixed and incubated for 20 minutes on ice. Preparations were then centrifuged (20,000 xg, 30 min, 4^{o}C) during which columns (Qiagen, Venlo, LI, Netherlands) were equilibrated with 10 mL QBT buffer (750 mM NaCl, 50 mM MOPS pH 7.0, 15% v/v isopropanol, 0.15% v/v Triton X-100). Supernatants were applied to the columns followed by 2x30 mL rinses with QC wash buffer (1.0 M NaCl, 50 mM MOPS pH 7.0, 15% v/v isopropanol). Lastly, DNA was eluted in 15 mL QF buffer (1.25 mM NaCl, 50 mM TrisHCl pH 8.5, 15% v/v isopropanol) and 10.5 mL of isopropanol were added to the eluate. The DNA solution was then centrifuged (15,000 xg, 30 min, 4^{o}C), the supernatant was discarded and the pellet was washed with 5 mL 70% EtOH and centrifuged (10,000 xg, 5 min, 4^{o}C). Finally, the supernatant was discarded, the pellet air dried and re-suspended in 300 μL 10 mM Tris pH 8.5; DNA was stored at -20^{o}C.

DNA was quantified using Quant-it Picogreen DNA assay kit (Life Technologies Inc., Burlington, ON, Canada), with commercial DNA as a standard. Vector preparations were thawed and diluted (10-100X) in 1X Tris-EDTA (TE) buffer. Samples were assayed in triplicate; 1 µL of undiluted, 10X diluted and 100X diluted DNA were added to 99 µL TE buffer in a black-bottom 96-well plate. Subsequently, 100 µL of Picogreen reagent were added to each well. Fluorescence readings were taken (excitation: 485 nm, emission: 520 nm) using FLUOstar Galaxy spectrophotometer (BMG Labtech, Ortenberg, Germany).

Restriction digest analysis was performed on 0.5 µg DNA for vector validation. Vector DNA was digested with 1 µL enzyme (psPAX2: Pst1, buffer 2; pMD2.G: NcoI, buffer 3; pTRIPZ: SalI, buffer 10) in a total volume of 20 µL at 37^{o}C for 1.5 hours. Following digest, 2 µL of loading dye (50% glycerol, 0.25% xylene cyanol FF) were added to each sample and run on 1% agarose gel, with λHindIII DNA as a reference. Ethidium Bromide was used as a visualizing agent and gels were imaged on ChemiDoc-It TS2 Imaging System (Ultra-Violet Products Ltd., Upland, CA, USA).

In a total volume of 100 µL, 2.8 µg pMD2.G and 5.3 µg psPAX2 were combined with or without 8 µg pTRIPZ vector (control or shRNA-containing). To this, 10 µL of 3M sodium acetate pH 5.2 and 200 µL 100% EtOH were added and samples were placed at -20^{o}C to precipitate DNA.

2.15 HEK293FT culture, transfection and viral collection

Frozen HEK293FT cells (passage number 5-8) were thawed and placed in complete growth medium, with changes every two days (complete growth medium: DMEM supplemented with 10% FBS, antibiotics (100 U/mL penicillin, 0.1 mg/mL streptomycin), 1mM sodium pyruvate, minimal essential medium with non-essential amino acids (MEM

NEAA) and 25 mM glucose, 400 μg/mL Geneticin (G418)). Each passage was performed with the addition of 1X TrypLE (Life Technologies Inc., Burlington, ON, Canada). After a minimum of four passages, cells were enumerated using a Neubauer hemocytometer and 800,000 cells were seeded per 100mm culture dish. Cells were grown to 70-90% confluence in preparation for transfection.

Cells were rinsed three times with 5 mL DMEM and antibiotics (100 U/mL penicillin, 0.1 mg/mL streptomycin), and subsequently placed in 7.5 mL DMEM with antibiotics for 2 hours at 37^{o}C. DNA preparations were centrifuged (18,000 xg, 15 min, 4^{o}C), the supernatants were discarded and pellets were left to air dry. Pellets were then re-suspended in 220 μL 0.1X TE buffer. To this, 116.7 μL of water and 37.7 μL of 2.0 M $CaCl_2$ were added. Finally, 380 μL of 2X HEPES Buffered Saline Solution (HBSS; 280 mM NaCl, 10 mM KCl, 1.5 mM Na_2HPO_4, 11 mM dextrose, 42 mM HEPES) were added drop wise with continuous mixing. The transfection cocktail was then added drop by drop around the plate, swirled once and incubated for 5 hours at 37^{o}C. After incubation, 800 μL FBS were added to the plate and cells were incubated overnight.

The following day, the transfection agents were removed and cells were rinsed four times with 5 mL complete growth medium (no G418) and placed in 5 mL medium. After 8 hours, medium was collected and stored at 4^{o}C, and 5 mL of fresh complete growth medium (no G418) were added and cells were returned to the incubator (37^{o}C) overnight. The following morning, media collection was repeated and combined with the collection from the previous day. Viral medium collection was centrifuged (150 xg, 5 min, 4^{o}C) and sterilized through a 0.45 μm filter. The samples were frozen at -80^{o}C until adipocyte infection.

Cells were subsequently placed in 8 mL complete growth medium (no G418) with 2 μg/mL doxycycline (DOX). DOX was replenished every day for 5 days with full medium

changes every second day. Transfection efficiency was visualized by comparing RFP fluorescent and phase images of the cells using an Axiovert S 100 microscope with an Axiocam camera attachment (Zeiss; Oberkochen, Germany).

2.16 Adipocyte infection

Filtered viral collections were thawed at room temperature and processed using PEG Virus Precipitation kit (BioVision, Milpitas, CA, USA). First, 5X polyethylene glycol (PEG) reagent was added and virus preparation was left overnight at 4^{o}C to precipitate the virus. The following day, the virus was centrifuged (3000 xg, 30 min, 4^{o}C), the supernatant removed and the virus re-suspended in re-suspension buffer (0.5 mL/viral collection). To this, 2 mL infection media (DMEM, 4 ng/mL polybrene) were added and the viral re-suspension was mixed. Media was removed from cells and 310 μL of viral re-suspension were added (60,000 cells/well, 24-well plate), and cells were incubated at 37^{o}C for 6 hours. After incubation, 310 μL of growth media were added to the cells and they were left to incubate overnight. The following day, viral re-suspension was removed and the cells were placed in 0.5 mL growth media for 24 hours. Knockdown was induced by adding 2 μg/mL DOX, which was replenished every day with full medium changes every second day. The infection was visualized by comparing RFP fluorescent and phase images of the cells using an Axiovert S 100 microscope with an Axiocam camera attachment (Zeiss; Oberkochen, Germany). Cells were harvested in Laemmli after 4-6 days of DOX treatment and assessed for knockdown via immunoblot analysis.

2.17 Immunohistochemistry

Cells were plated, differentiated and stimulated as described above on three coverslips per experimental dish. After stimulation, cells were rinsed twice with 1 mL 1X

PBS and incubated in 2 mL 3.7% paraformaldehyde for 20 minutes at room temperature. Following fixation, cells were rinsed twice with 1 mL 1X PBS and incubated in 2 mL 0.2% Triton X-100 for 10 minutes at room temperature. Subsequently, cells were rinsed three times with 1mL 1X PBS and incubated in 2 mL blocking solution (1% FBS) for 30 minutes at room temperature. Coverslips were then removed from each plate, rinsed three times through 1X PBS and placed face-up in a humid chamber. Next, 50 µL of PRAJA2 antibody (1:50 rabbit anti-PRAJA2; Sigma-Aldrich, St. Louis, MO, USA) or antibody dilution buffer (3% BSA in 1X PBS) were added to the sample or control respectively and incubated in the humid chamber at 37^{o}C for 45 minutes. Once again, coverslips were rinsed and incubated in 50 µL anti-rabbit secondary antibody (Alexa Fluor 488 anti-rabbit IgG antibody (1:100; Life Technologies Inc., Burlington, ON, Canada) at 37^{o}C for 45 minutes. Rinses and antibody incubations were repeated consecutively with PKAR2 (1:50; mouse anti-PKAR2; Abcam, Cambridge, England, UK) and Cy3-anti mouse IgG (1:100; Jackson ImmunoResearch Laboratories, West Grove, PA, USA). Next, coverslips were rinsed and incubated with 50 µL of 1 µg/mL Hoechst dye for 10 minutes at room temperature. Finally, coverslips were rinsed and mounted facedown on glass slides with 15 µL Mowiol/coverslip.

Cells were visualized and photographed (400X magnification) with a Zeiss Axio Imager.M1 microscope equipped with an Axiocam HRm digital camera (Zeiss, Oberkochen, Germany). Two random fields were photographed for each of the two coverslips used per treatment. The following filters were applied Alexa fluor 488 (excitation: 495 nm, emission: 579 nm), Hoechst (excitation: 359 nm, emission: 467 nm), Cy3 (excitation: 578 nm, emission: 603 nm). Analysis was performed by assessing the staining for each cell in the field of view for localization from the merged images.

2.18 Statistical analysis

A one-way ANOVA was used to establish significance within each experiment. Student-Newman-Keuls was used as a post-hoc test to assess differences between multiple means (Instat, version 3.05; Graphpad). Additionally, a t-test was performed to establish significance within each time point (Excel 2010, version 14.0.7; Microsoft). Pearson's correlation was used to assess linear dependence (Instat, version 3.05; Graphpad). Pvalues <0.05 were considered significant.

3. RESULTS

3.1 TSH or isoproterenol stimulate lipolysis in human primary differentiated adipocytes

To confirm the lipolytic response of human primary differentiated adipocytes via stimulation of TSHR or β-adrenergic receptors as previously shown by our research group, these cells were stimulated with TSH or isoproterenol (Gagnon et al., 2010). Primary differentiated adipocytes were stimulated for 4 hours with 5mU/ml TSH, 50mU/mL TSH, 1μM isoproterenol or vehicle. All three treatments were able to stimulate release and accumulation of NEFA and glycerol within the culture media. NEFA release showed a dose-dependent response for TSH stimulation with up to a 3-fold increase when compared to the control condition (Figure 2A). Similar results were seen for glycerol release upon stimulation with TSH or isoproterenol, with up to a 7-fold increase when compared to the control condition (Figure 2B). Intracellular triglycerides showed no significant difference between conditions, indicating an equal degree of differentiation across experimental conditions (Figure 2C). Data were normalized to cellular protein content as determined by the modified Lowry assay.

3.2 PRAJA2 is expressed in primary human differentiated adipocytes

Performance of the commercially available PRAJA2 antibody was assessed in this primary cellular model. The antibody was used to measure protein expression of PRAJA2 in untreated primary human differentiated adipocytes. The PRAJA2 antibody showed a clear signal that was proportional to the amount of solubilized cellular protein (10-50 μg) (Figure 3A, B). The signal was detected at a molecular weight of ~120kDa, consistent with the

A)

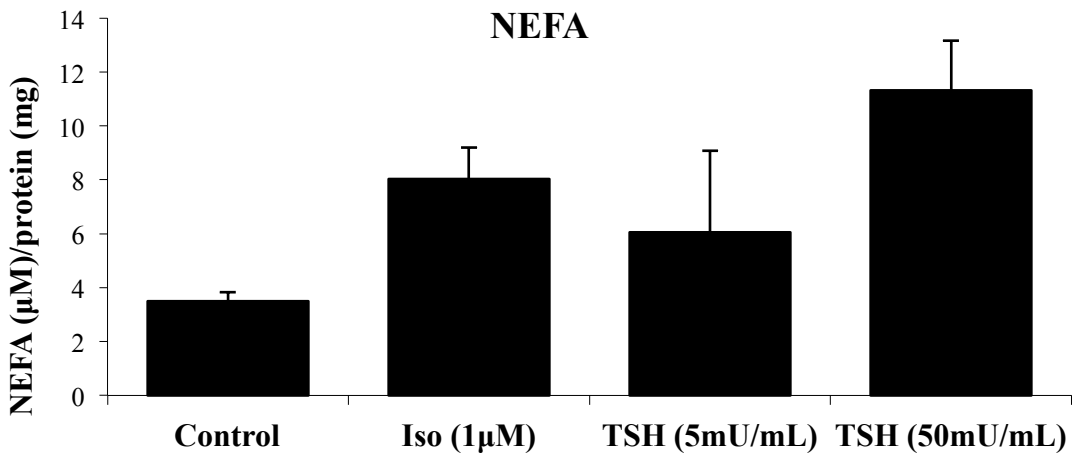
NEFA
NEFA (µM)/protein (mg)
14
12
10
8
6
4
2
0
Control
Iso (1µM)
TSH (5mU/mL)
TSH (50mU/mL)

B)

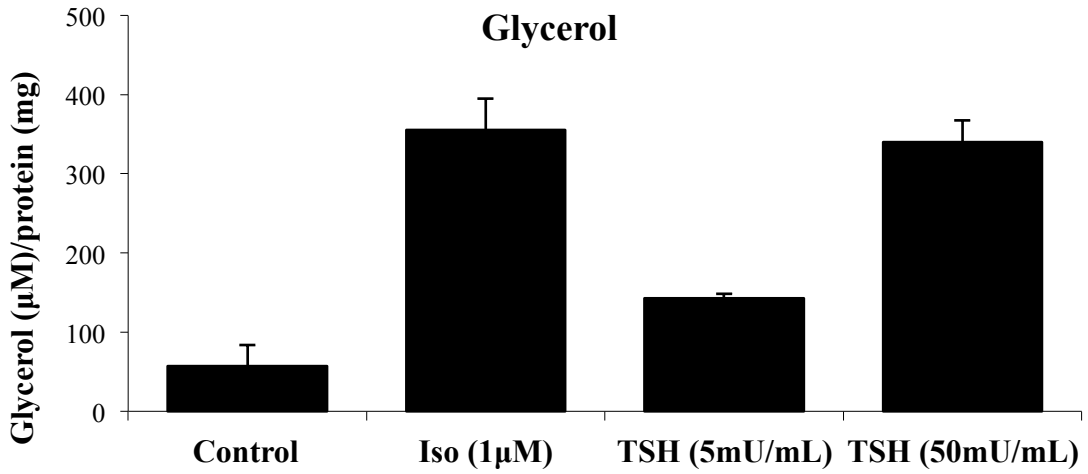
Glycerol
Glycerol (µM)/protein (mg)
500
400
300
200
100
0
Control
Iso (1µM)
TSH (5mU/mL)
TSH (50mU/mL)

C)

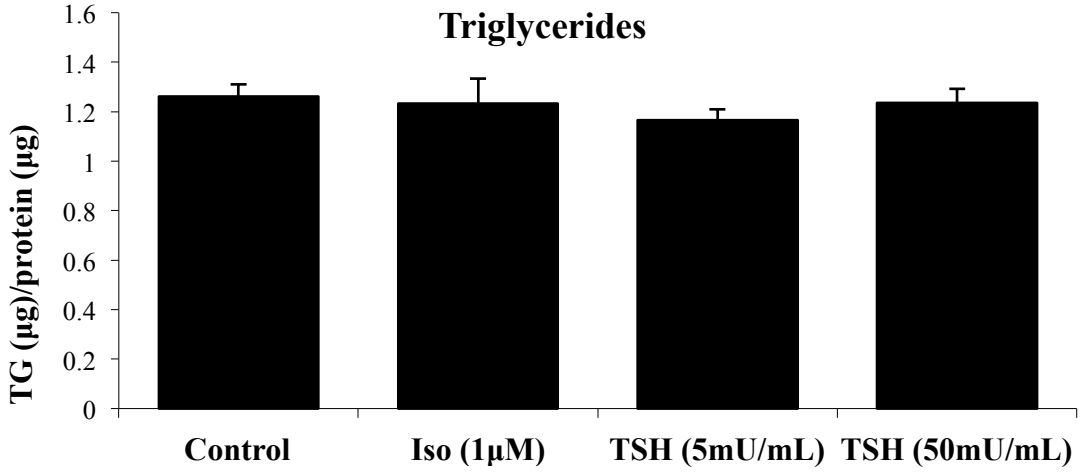
Triglycerides
TG (µg)/protein (µg)
1.6
1.4
1.2
1
0.8
0.6
0.4
0.2
0
Control
Iso (1µM)
TSH (5mU/mL)
TSH (50mU/mL)

Figure 2. ***TSH and isoproterenol stimulate lipolysis in human primary differentiated adipocytes.*** Human primary differentiated adipocytes were treated with 1μM isoproterenol, 5mU/mL TSH, 50mU/mL TSH or vehicle for 4hrs. Conditioned medium was analyzed for non-esterified fatty acids **(A)** and glycerol **(B)** release. Triglycerides were extracted and analyzed **(C)** as an indicator of differentiation. Values from 2 separate patients are expressed as mean ± range after normalizing to cellular protein.

A)

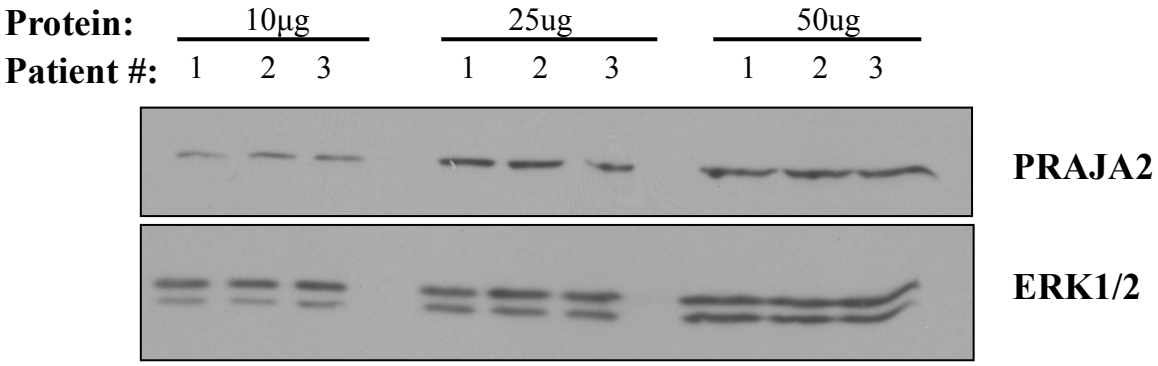
Protein:
10µg
25ug
50ug
Patient #:
1 2 3
1 2 3
1 2 3
PRAJA2
ERK1/2

B)

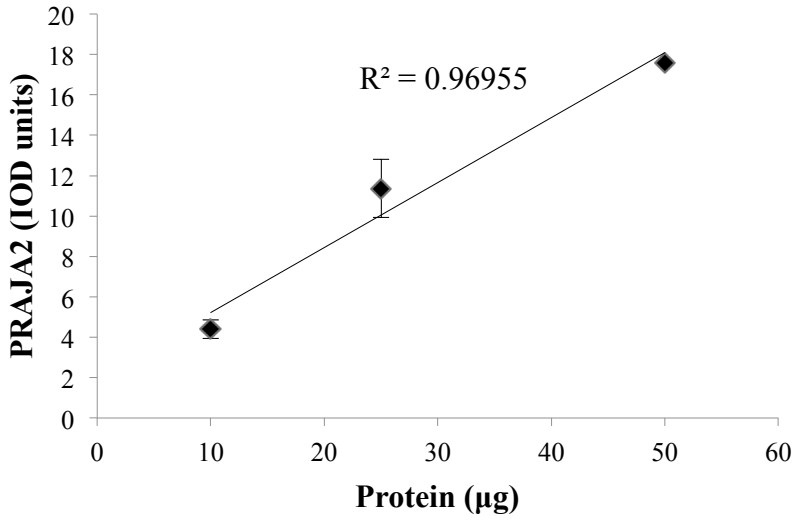
R² = 0.96955
PRAJA2 (IOD units)
Protein (µg)
0
2
4
6
8
10
12
14
16
18
20
0
10
20
30
40
50
60

C)

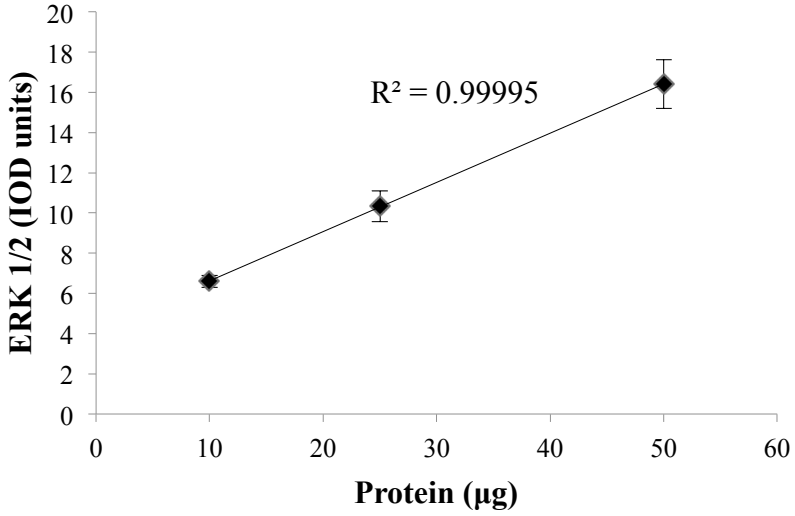
R² = 0.99995
ERK 1/2 (IOD units)
Protein (µg)
0
2
4
6
8
10
12
14
16
18
20
0
10
20
30
40
50
60

Figure 3. ***PRAJA2 is expressed in primary human differentiated adipocytes.*** Solubilized protein from untreated human primary differentiated adipocytes was separated by SDS-PAGE and immunoblotted for PRAJA2 and ERK1/2 (loading control). An immunoblot of 3 patient samples (1-3) showing PRAJA2 and ERK1/2 with increasing amounts of solubilized protein is presented **(A)**. Densitometry data from 3 separate patient samples for PRAJA2 **(B)** and ERK1/2 **(C)** expressed as mean ± SEM. Pearson's correlation was used to assess linear dependence (R^2: coefficient of determination).

literature (Lignitto et al., 2011). ERK1/2 was used as a loading control and showed a parallel response proportional to the amount of solubilized cellular protein (Figure 3A, C).

3.3 PRAJA2 is equally expressed in primary human preadipocytes and differentiated adipocytes

PRAJA2 expression was compared in primary human preadipocytes and primary human differentiated adipocytes. Cells were harvested after being subjected to either differentiation medium for 14 days (adipocytes) or normal growth medium for 14 days (preadipocytes). The cellular lysates were analyzed for PRAJA2 via immunoblot, with fatty acid synthase (FAS) as a marker of differentiation and Coomassie staining as a loading control (Figure 4A). Densitometric analysis of the immunoblots showed a significant increase in FAS in adipocytes (Figure 4B; $p<0.001$). PRAJA2 was detected in both preadipocytes and differentiated adipocytes, without any difference in expression (Figure 4C). Protein loading was equal for all samples, as assessed by Coomassie staining (Figure 4 D).

3.4 TSH or isoproterenol stimulation does not alter PRAJA2 expression at the mRNA level in human primary differentiated adipocytes

Given the involvement of PRAJA2 in PKA regulation, and its increased expression in TSH-responsive thyroid cancer cells, it was investigated whether there were transcriptional effects of TSH or isoproterenol on PRAJA2 gene expression. Primary human differentiated adipocytes were stimulated for 2, 4, or 24 hours, with 5mU/mL TSH, 1μM isoproterenol or vehicle, and then harvested and processed for qPCR analysis of mRNA. PRAJA2 transcript levels were assessed with 18S as an internal control. PRAJA2 mRNA was detected in

A)

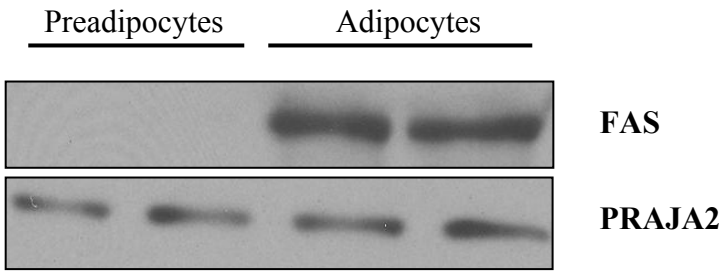
Preadipocytes
Adipocytes
FAS
PRAJA2

B)

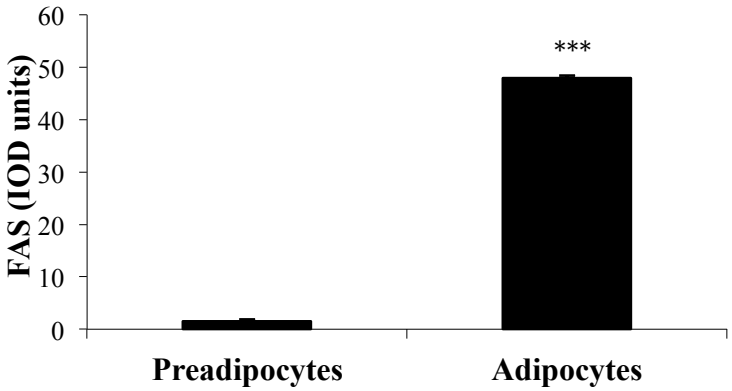
60
50
40
30
20
10
0
FAS (IOD units)
***
Preadipocytes
Adipocytes

C)

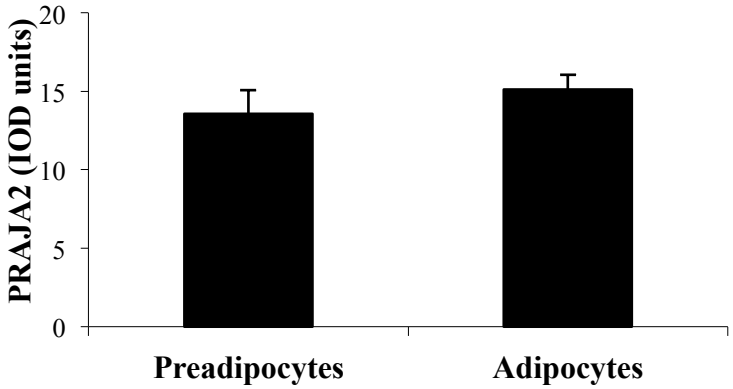
20
15
10
5
0
PRAJA2 (IOD units)
Preadipocytes
Adipocytes

D)

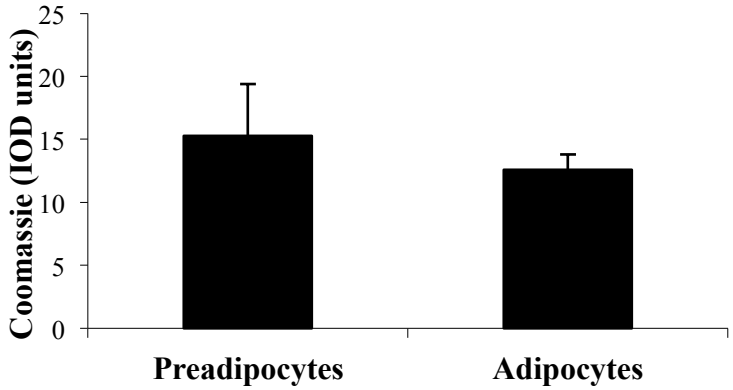
25
20
15
10
5
0
Coomassie (IOD units)
Preadipocytes
Adipocytes

Figure 4. ***PRAJA2 is equally expressed in primary human preadipocytes and differentiated adipocytes.*** Human primary preadipocytes and differentiated adipocytes were harvested at day 14. Cellular proteins were separated by SDS-PAGE and immunoblotted for PRAJA2 and fatty acid synthase (FAS, differentiation marker). Coomassie staining was used to assess loading. A representative immunoblot showing PRAJA2 and FAS is presented **(A)**. Densitometric data from 3 separate patient samples for FAS **(B)**, PRAJA2 **(C)** and Coomassie stain **(D)** are expressed as mean ± SEM, *** indicates $p<0.001$, determined by one-way ANOVA and the Student-Newman-Keuls test.

adipocytes, and levels did not change following stimulation with TSH (Figure 5A) or isoproterenol (Figure 5B).

3.5 TSH or isoproterenol stimulation does not alter PRAJA2 protein expression in primary differentiated adipocytes

PRAJA2 protein levels were measured basally and upon TSH or isoproterenol stimulation to assess potential post-transcriptional regulation. Primary human differentiated adipocytes were stimulated for 4, 6, or 24 hours, with 5mU/mL TSH, 1μM isoproterenol or vehicle. Cellular lysates were analyzed for PRAJA2 by immunoblot analysis, with ERK 1/2 as a loading control (Figure 6A, 7A). PRAJA2 was detectable at all time points. There was no significant difference following TSH stimulation, compared to the control (Figure 6B). Additionally, there was no significant difference following isoproterenol stimulation, compared to the control (Figure 7B). A longer time course up to 48 hours showed no significant differences (Figure 8A). There were no significant differences in the ERK1/2 loading controls.

3.6 Isoproterenol increases PKA-specific phosphorylation of PRAJA2-associated proteins

PKA was shown to be phosphorylated by PRAJA2 in studies that overexpressed FLAG-PRAJA2 in HEK293 cells (Lignitto et al., 2011). Therefore, it was assessed if endogenous PRAJA2 was phosphorylated by PKA. Primary human differentiated adipocytes were stimulated for 5, 15 or 30 min, with 1μM isoproterenol or vehicle. Cellular lysates were collected and PRAJA2 was immunoprecipitated using the PRAJA2 antibody. Immunoprecipitates were then immunoblotted using pPKA substrate antibody to assess

A)

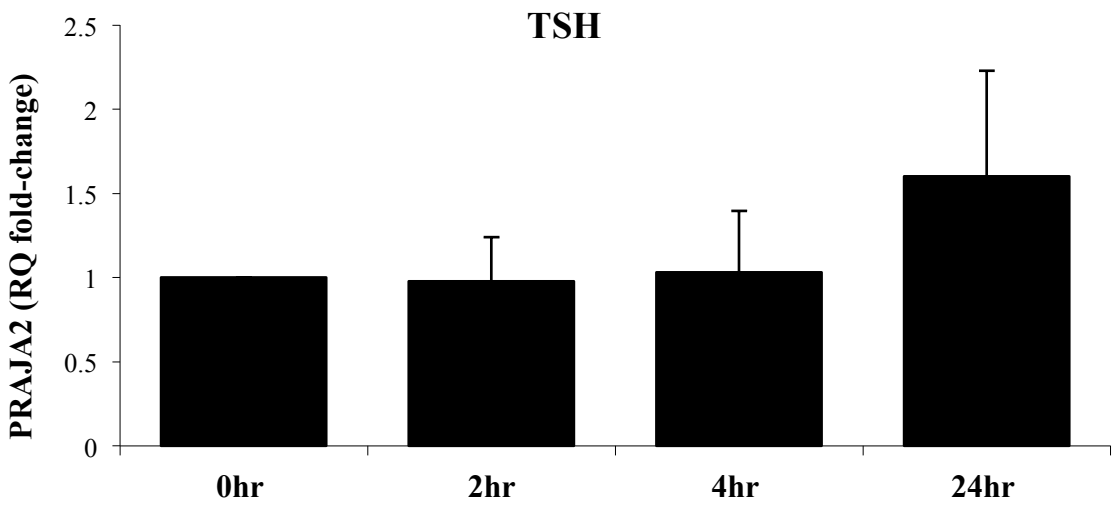
TSH
PRAJA2 (RQ fold-change)
2.5
2
1.5
1
0.5
0
0hr
2hr
4hr
24hr

B)

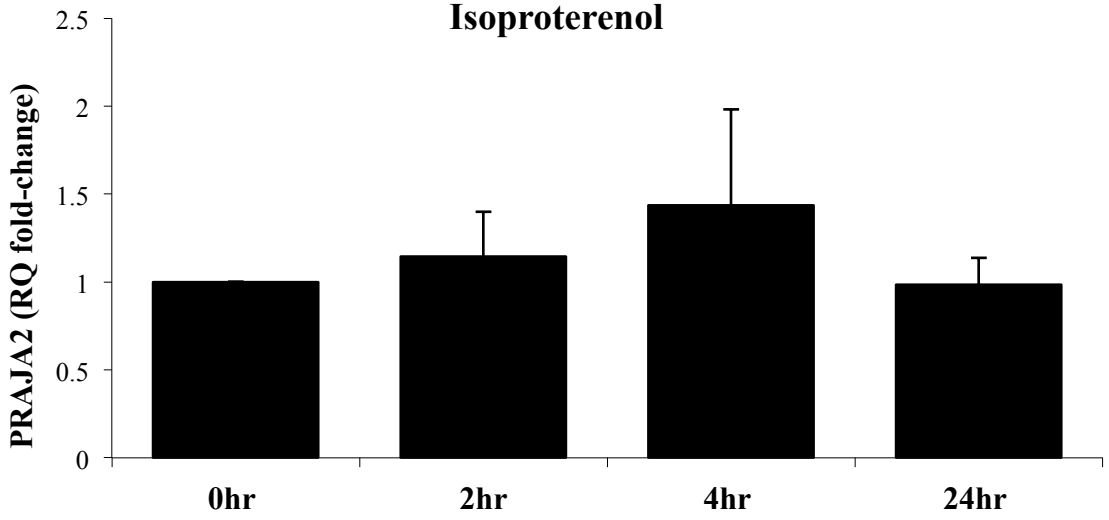
Isoproterenol
PRAJA2 (RQ fold-change)
2.5
2
1.5
1
0.5
0
0hr
2hr
4hr
24hr

Figure 5. ***TSH or isoproterenol stimulation does not alter PRAJA2 mRNA expression in differentiated adipocytes.*** Human primary differentiated adipocytes were treated with 5mU/mL TSH **(A)**, 1μM isoproterenol **(B)** or vehicle for 2, 4 or 24hrs. Cellular mRNA was extracted using Qiazol reagent and analyzed for PRAJA2 expression by qPCR with 18S as an internal control. Data from 4 separate patient samples are expressed as mean (fold of control) ±SEM. A one-way ANOVA was used to assess statistical significance between conditions; no significant differences were found.

A)

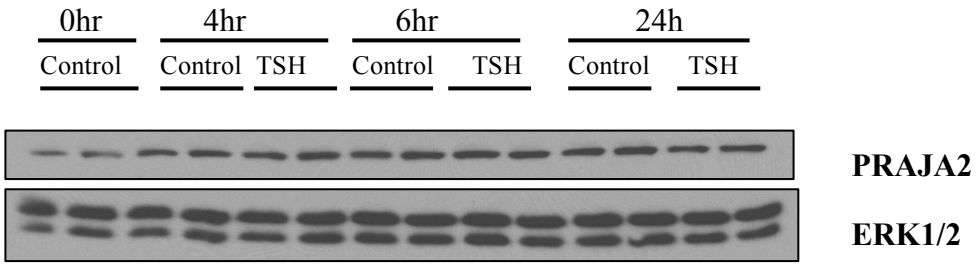
0hr
4hr
6hr
24h
Control
Control
TSH
Control
TSH
Control
TSH
PRAJA2
ERK1/2

B)

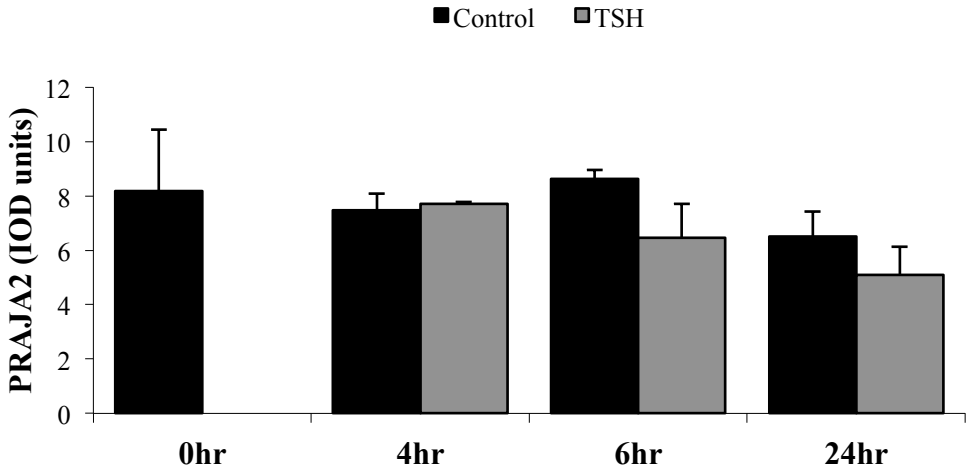
Control
TSH
PRAJA2 (IOD units)
0
2
4
6
8
10
12
0hr
4hr
6hr
24hr

C)

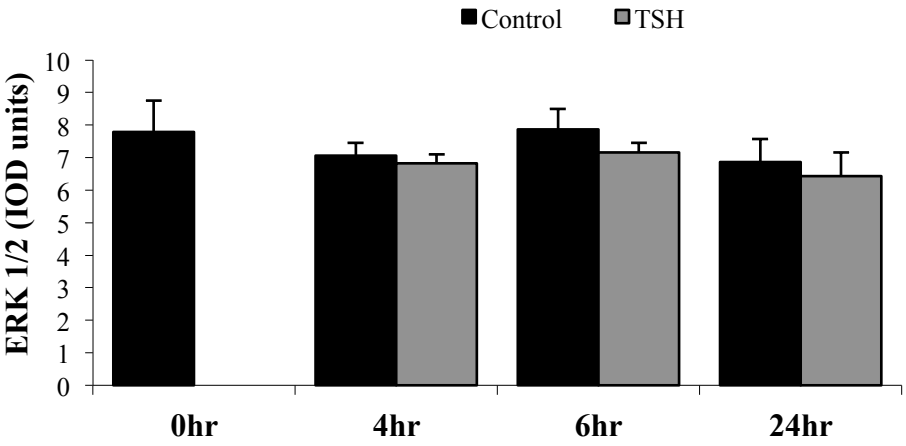
Control
TSH
ERK 1/2 (IOD units)
0
1
2
3
4
5
6
7
8
9
10
0hr
4hr
6hr
24hr

Figure 6. ***TSH stimulation does not alter PRAJA2 protein expression in differentiated adipocytes.*** Human primary differentiated adipocytes were treated with 5mU/mL TSH or vehicle for 4, 6 or 24hrs. Cellular proteins were separated by SDS-PAGE and immunoblotted for PRAJA2 and ERK1/2 (loading control). A representative immunoblot showing PRAJA2 and ERK1/2 is presented **(A)**. Densitometry data from 3 separate patient samples for PRAJA2 **(B)** and ERK1/2 **(C)** are expressed as mean ± SEM. A one-way ANOVA was used to assess statistical significance between conditions; no significant differences were found.

A)

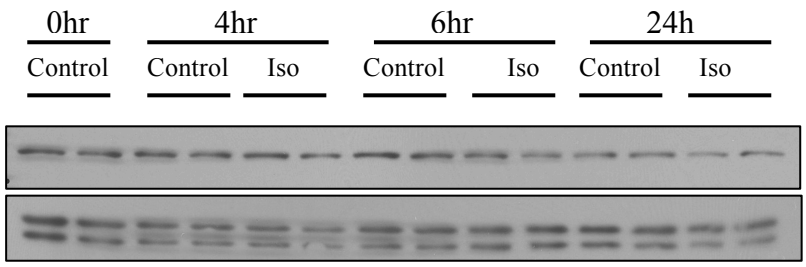
0hr
4hr
6hr
24h
Control
Control
Iso
Control
Iso
Control
Iso
PRAJA2
ERK1/2

B)

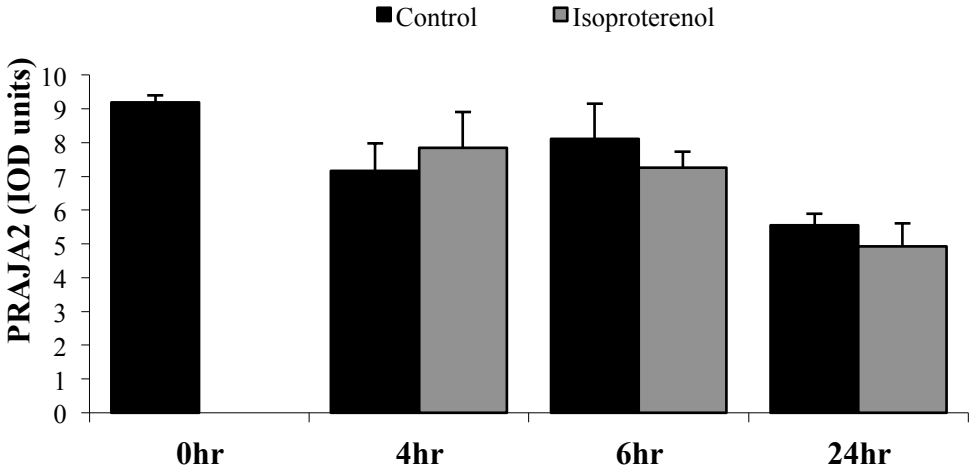
Control
Isoproterenol
PRAJA2 (IOD units)
0
1
2
3
4
5
6
7
8
9
10
0hr
4hr
6hr
24hr

C)

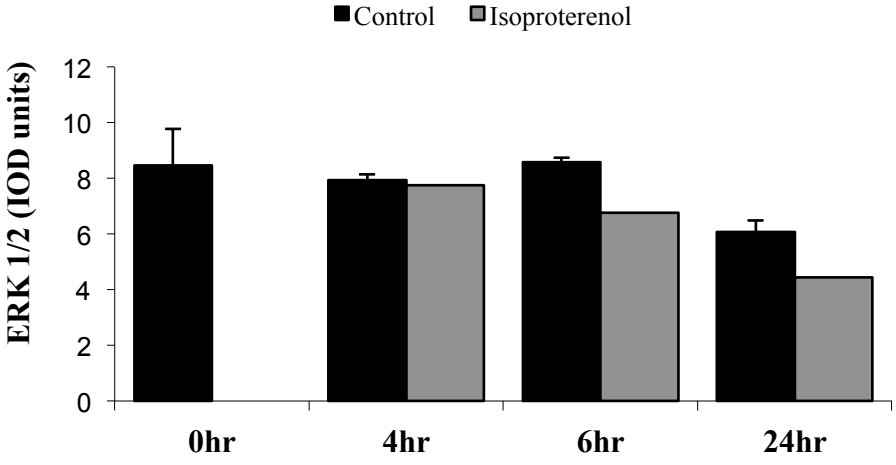
Control
Isoproterenol
ERK 1/2 (IOD units)
0
2
4
6
8
10
12
0hr
4hr
6hr
24hr

Figure 7. ***Isoproterenol stimulation does not alter PRAJA2 protein expression differentiated adipocytes.*** Human primary differentiated adipocytes were treated with 1μM isoproterenol or vehicle for 4, 6 or 24hrs. Cellular proteins were separated by SDS-PAGE and immunoblotted for PRAJA2 and ERK1/2 (loading control). A representative immunoblot showing PRAJA2 and ERK1/2 is presented **(A)**. Densitometry data from 3 separate patient samples for PRAJA2 **(B)** and ERK1/2 **(C)** are expressed as mean ± SEM. A one-way ANOVA was used to assess statistical significance between conditions; no significant differences were found.

A)

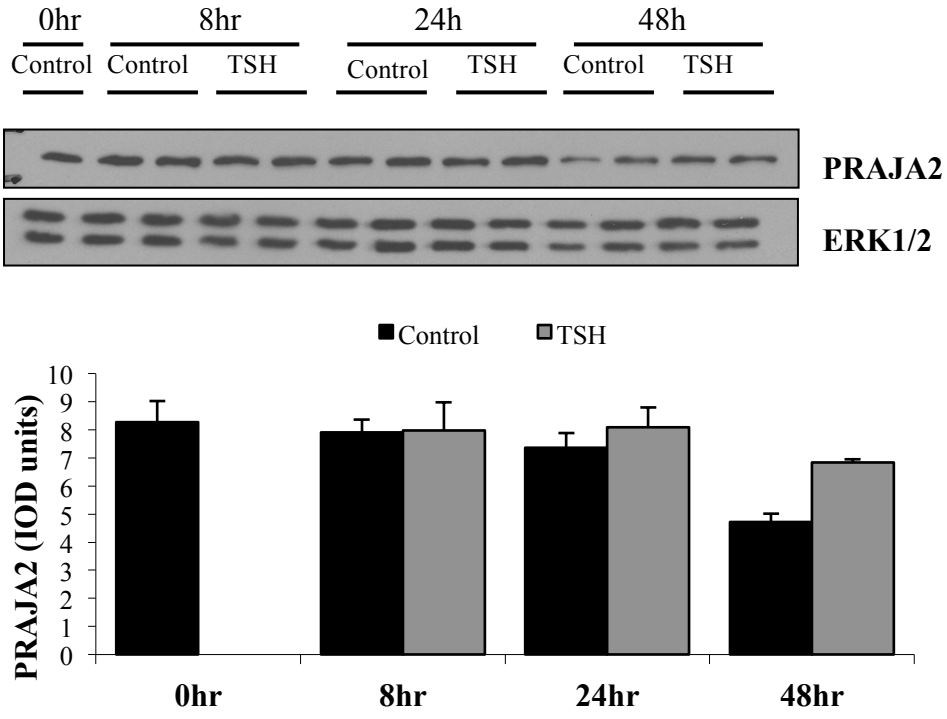
0hr
8hr
24h
48h
Control
Control
TSH
Control
TSH
Control
TSH
PRAJA2
ERK1/2
Control
TSH
PRAJA2 (IOD units)
0
1
2
3
4
5
6
7
8
9
10
0hr
8hr
24hr
48hr

B)

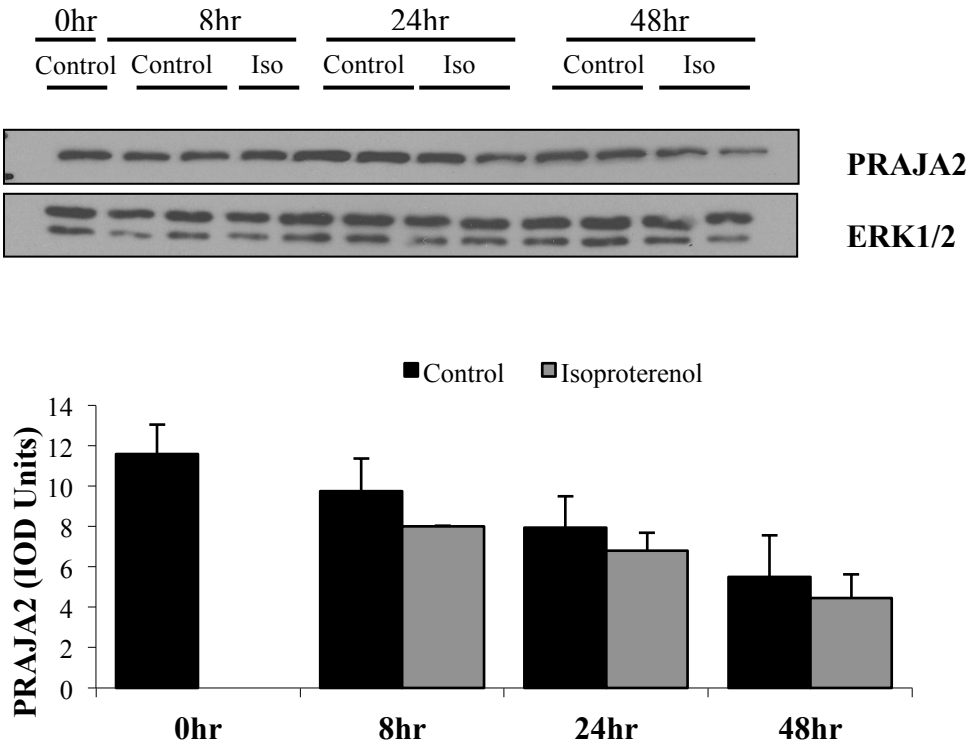
0hr
8hr
24hr
48hr
Control
Control
Iso
Control
Iso
Control
Iso
PRAJA2
ERK1/2
Control
Isoproterenol
PRAJA2 (IOD Units)
0
2
4
6
8
10
12
14
0hr
8hr
24hr
48hr

Figure 8. ***TSH or isoproterenol stimulation at later time points does not alter PRAJA2 protein expression in differentiated adipocytes.*** Human primary differentiated adipocytes were treated with 5mU/mL TSH **(A)**, 1μM isoproterenol **(B)** or vehicle for 8, 24 or 48hrs. Cellular proteins were separated by SDS-PAGE and immunoblotted for PRAJA2 and ERK1/2 (loading control). Representative immunoblots show PRAJA2 and ERK1/2. Densitometry data from 3 separate patient samples for PRAJA2 are expressed as mean ± SEM. A one-way ANOVA was used to assess statistical significance between conditions; no significant differences were found.

phosphorylated PKA substrates, as well as PRAJA2 antibody to assess immunoprecipitation efficiency (Figure 9A). In these studies, a faint band was visible at 122kDa, as interpolated via standard curve analysis. Phosphorylation state of this 122kDa protein appears responsive to isoproterenol stimulation, with a significant response noted at the 5 minute time point (Figure 9A, B; p=0.05). In addition to the 122kDa band a second, band of interest appears at 69kDa. This 69kDa protein co-immunoprecipitates with PRAJA2 and appears to be a PKA-phosphorylation target. Its phosphorylation seems highly responsive to isoproterenol stimulation at all time points, with statistical significance at the 15 minute time point (Figure 9A, C; p=0.01).

3.7 TSH does not alter PKA-specific phosphorylation of PRAJA2-associated proteins

Primary human differentiated adipocytes were stimulated for 5 or 15 min, with 5mU/mL TSH or vehicle. Cellular lysates were collected and immunoprecipitated using the PRAJA2 antibody. Immunoprecipitates were then immunoblotted using pPKA substrate antibody to assess phosphorylated PKA substrates, as well as PRAJA2 antibody to assess immunprecipitation efficiency (Figure 10A). Again the 69kDa protein co-immunoprecipitates with PRAJA2 and is detected as a PKA-phosphorylation target; however, phosphorylation is not altered following TSH stimulation. Densitometric analysis of this band shows no significant difference between treatments (Figure 10B).

3.8 Immunoprecipitation of pPKA substrates to detect PRAJA2 phosphorylation

PKA-specific phosphorylation of PRAJA2 was assessed by determining its presence in pPKA substrate antibody immunoprecipitates. Primary human differentiated adipocytes were stimulated for 5, 15 or 30min, with 1μM isoproterenol or vehicle.

A)

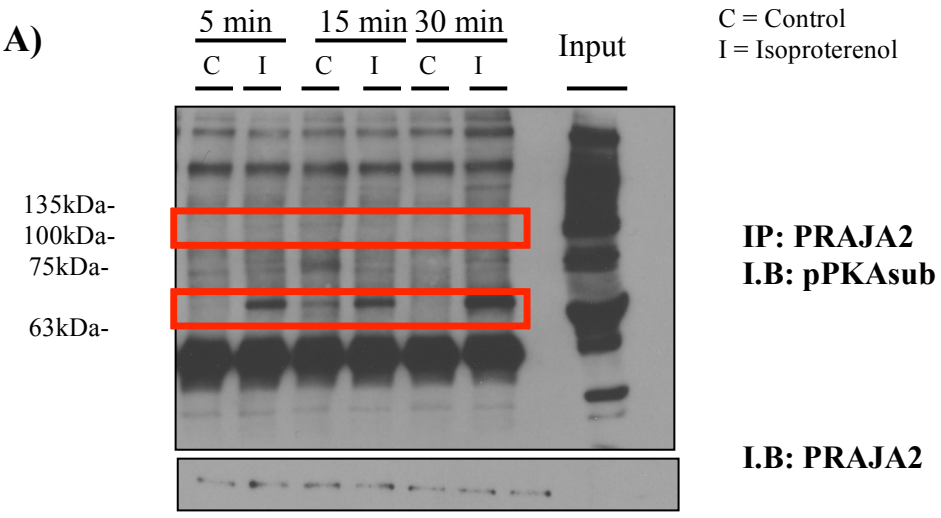
5 min
15 min
30 min
Input
C
I
C
I
C
I
C = Control
I = Isoproterenol
135kDa-
100kDa-
75kDa-
63kDa-
IP: PRAJA2
I.B: pPKAsub
I.B: PRAJA2

B)

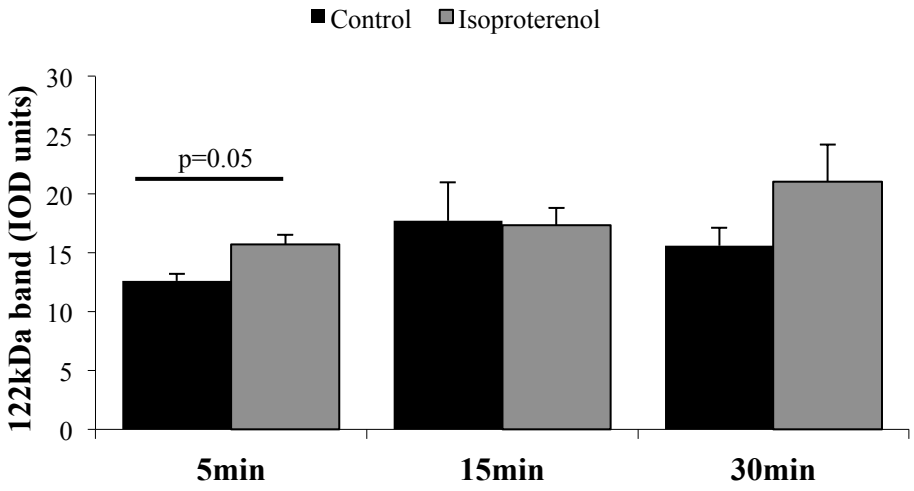
Control
Isoproterenol
122kDa band (IOD units)
30
25
20
15
10
5
0
p=0.05
5min
15min
30min

C)

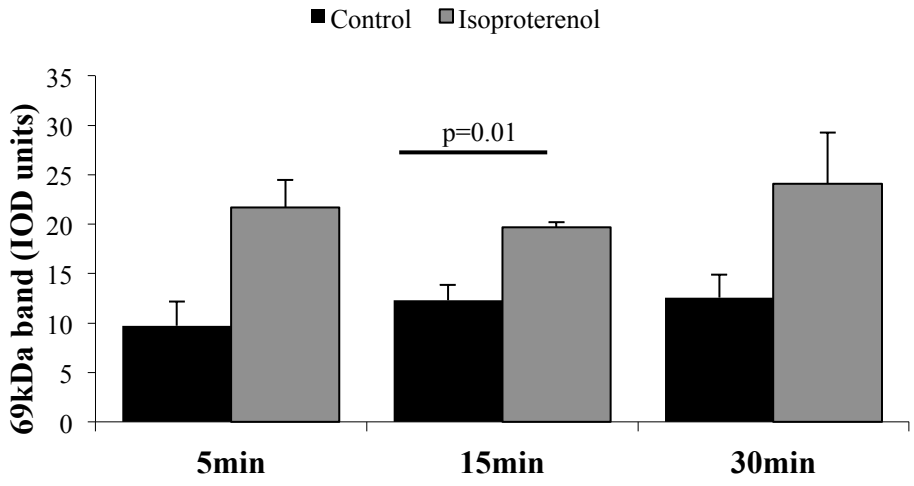
Control
Isoproterenol
69kDa band (IOD units)
35
30
25
20
15
10
5
0
p=0.01
5min
15min
30min

Figure 9. ***Isoproterenol increases PKA-specific phosphorylation PRAJA2-associated proteins.*** Human primary differentiated adipocytes were treated with 1μM isoproterenol or vehicle for 5, 15 or 30mins. Cellular lysates were immunoprecipitated using anti PRAJA2 antibody. Proteins were separated by SDS-PAGE and immunoblotted for pPKAsub and PRAJA2 (IP control). A representative immunoblot of pPKAsub shows PKA phosphorylation events in response to stimulation (122kDa and 69kDa), and PRAJA2 control **(A)**. Densitometry data from 3-4 separate patient samples for 122kDa **(B)** and 69kDa band **(C)** are expressed as mean ± SEM. Significance determined by paired t-test within each time point.

A)

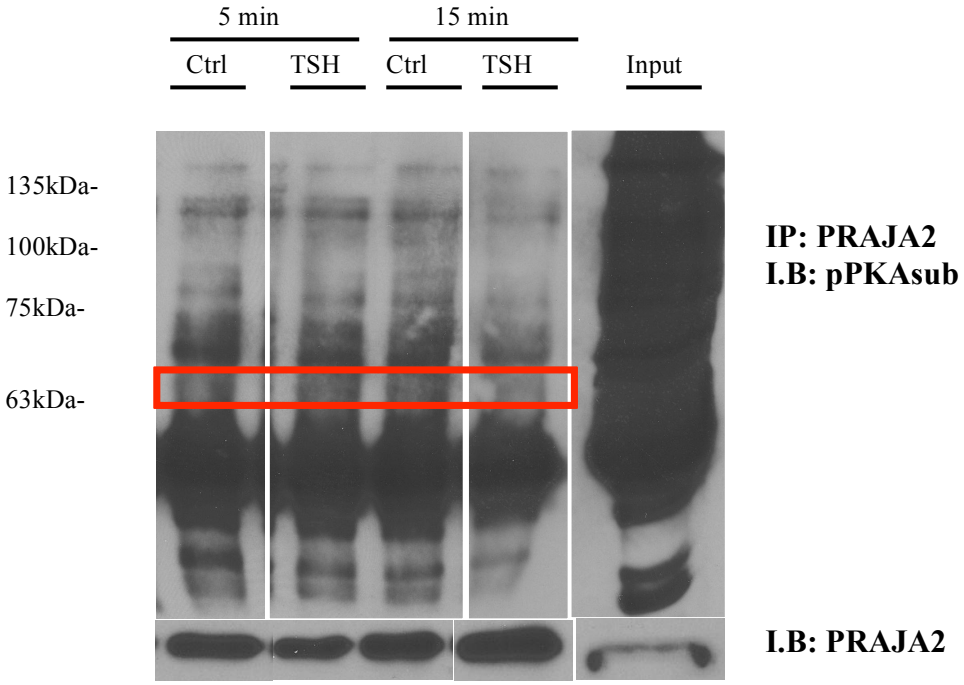
5 min
15 min
Ctrl
TSH
Ctrl
TSH
Input
135kDa-
100kDa-
75kDa-
63kDa-
IP: PRAJA2
I.B: pPKAsub
I.B: PRAJA2

B)

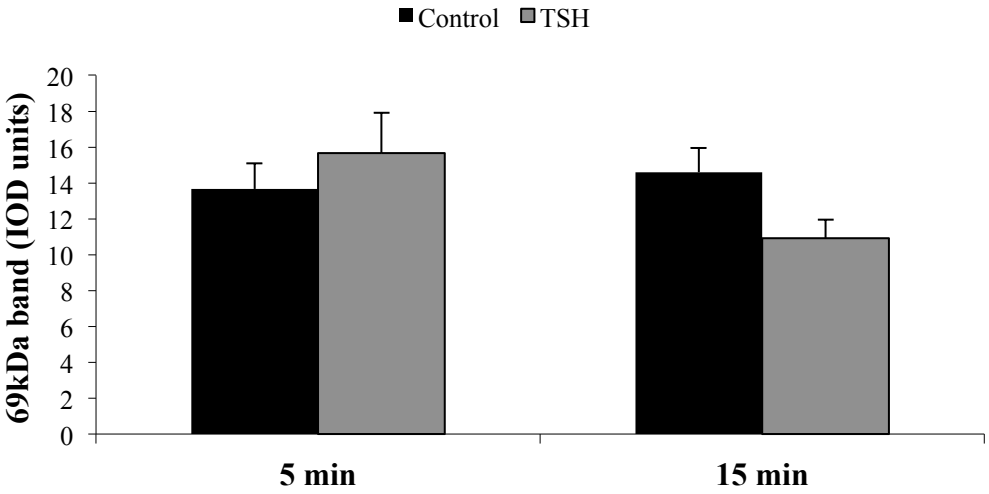
Control
TSH
69kDa band (IOD units)
20
18
16
14
12
10
8
6
4
2
0
5 min
15 min

Figure 10. ***TSH does not increase PKA-specific phosphorylation PRAJA2-associated proteins.*** Human primary differentiated adipocytes were treated with 5mU/mL TSH or vehicle for 5 or 15 mins. Cellular lysates were immunoprecipitated using PRAJA2 antibody. Proteins were separated by SDS-PAGE and immunoblotted for pPKAsub and PRAJA2 (IP control). A representative immunoblot of pPKAsub shows PKA phosphorylation events in response to stimulation (69kDa), and PRAJA2 control **(A)**. Densitometry data from 3 separate patient samples for 69kDa band **(B)** are expressed as mean ± SEM. Significance determined by paired t-test within each time point; no significant differences were found.

Cellular lysates were collected and immunoprecipitated using the pPKAsub antibody. Immunoprecipitated samples were then analyzed for PRAJA2 by immunoblot analysis, as well as pPKAsub to assess PKA activity and extent of immunoprecipitation (Figure 11). However, phosphorylated PRAJA2 was not detected in this series of immunoprecipitation experiments.

3.9 Interaction between PKAR2 and PRAJA2

PKAR2 interacts with PRAJA2 under basal conditions. Disassembly of this complex and degradation of PKAR2 by the proteasome occur following cellular stimulation (Hedrick et al., 2013; Lignitto et al., 2011). Attempts were made to assess whether PKAR2-PRAJA2 interaction would decrease following cellular stimulation in our experimental model. Primary human differentiated adipocytes were stimulated for 5, 15 or 30 min, with 1μM isoproterenol or vehicle. Cellular lysates were immunoprecipitated using the PKAR2 antibody. Immunoprecipitates were then analyzed for PRAJA2 by immunoblot analysis. No band corresponding to PKAR2 was seen in the immunoprecipitated samples (Figure 12). immunoprecipitation efficiency of PKAR2 could not be assessed due to immunoblot interference by the antibody IgG band (Figure 12).

The direct immunoprecipitation kit by Pierce was used in an attempt to eliminate the antibody following the immunoprecipitation step, to prevent the IgG interference. PKAR2 antigen was detected in the input sample but not in the immunoprecipitates. Some antigen was noted in the post-IP flow through suggesting it might not have all been captured by the antibody. Next the pH of the elution buffer was varied to assess if antigen was remaining in complex with the antibody, however no antigen was detected in this series of elutions. Finally, the resin was collected and denatured; from this IgG was detected but no

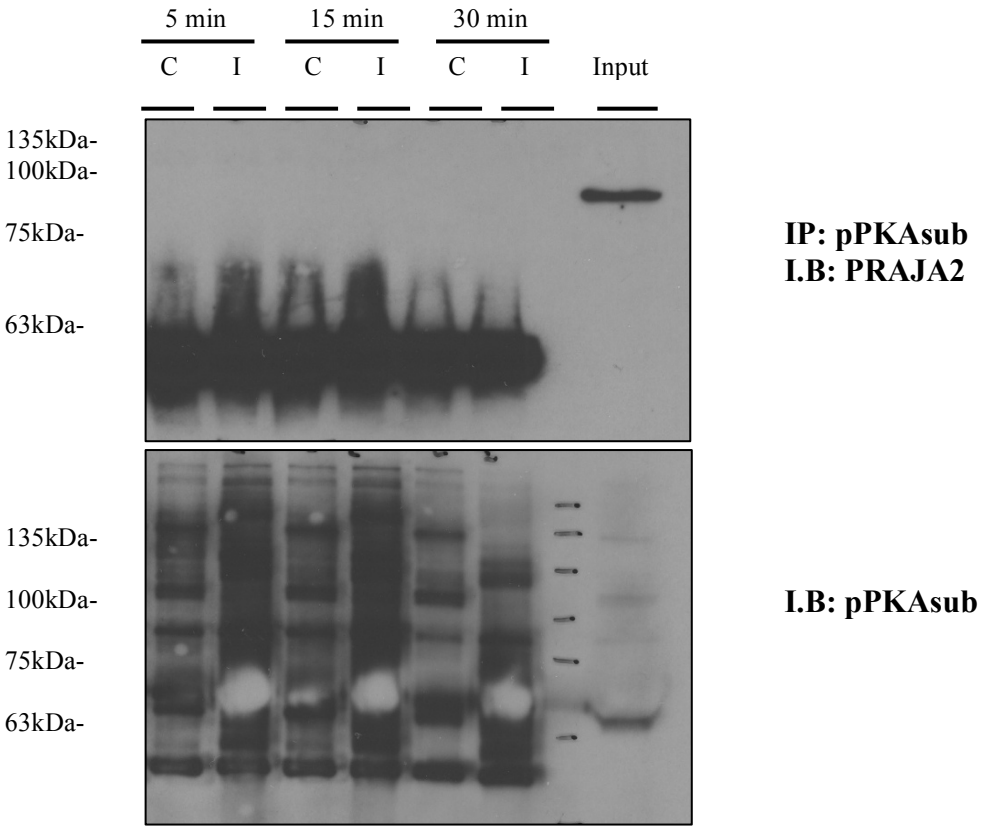
5 min
15 min
30 min
C
I
C
I
C
I
Input
135kDa-
100kDa-
75kDa-
63kDa-
IP: pPKAsub
I.B: PRAJA2
135kDa-
100kDa-
75kDa-
63kDa-
I.B: pPKAsub

Figure 11. ***Immunoprecipitation of pPKAsub to detect PRAJA2 phosphorylation.*** Human primary differentiated adipocytes were treated with 1μM isoproterenol or vehicle for 5, 15 or 30 mins. Cellular lysates were immunoprecipitated using anti-phosphoPKA substrate antibody. Proteins were separated by SDS-PAGE and immunoblotted for PRAJA2 and pPKAsub (IP control). A representative immunoblot shows PRAJA2 and pPKAsub immunoblots. Data from 3 separate patient samples were assessed.

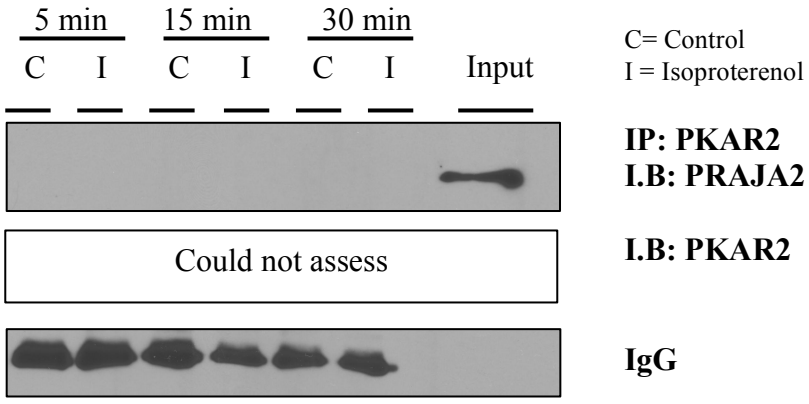
5 min
15 min
30 min
C
I
C
I
C
I
Input
C= Control
I = Isoproterenol
IP: PKAR2
I.B: PRAJA2
Could not assess
I.B: PKAR2
IgG

Figure 12. ***Immunoprecipitation of PKAR2 to detect PRAJA2 association.*** Human primary differentiated adipocytes were treated with 1μM isoproterenol or vehicle for 5, 15 or 30mins. Cellular lysates were immunoprecipitated using anti-PKAR2 antibody. Proteins were separated by SDS-PAGE and immunoblotted for PRAJA2. A representative immunoblot shows PRAJA2. Data from 2 separate patient samples were assessed.

antigen. Based on this series of troubleshooting attempts, it is believed that the antibody successfully bound the resin but in this state was unable to bind the antigen, potentially due to its orientation upon conjugation to the resin.

3.10 PRAJA2/PKAR2 localization analysis via immunohistochemistry

Next, the potential cellular localization of PRAJA2 and PKAR2 basally and in response to isoproterenol was analyzed. Lignitto *et al.,* 2011 showed partial co-localization of PRAJA2 and PKAR2 with endogenous proteins in neuroblastoma (SHSY) cells. When they overexpressed FLAG-PRAJA2, the endogenous PKAR2 underwent intracellular redistribution from the golgi-centrosome to the cytoplasm and plasma membrane. Primary human differentiated adipocytes were stimulated for 5, 15 and 30 min with 1μM isoproterenol or vehicle. Cells were then fixed, permeablilized, blocked and probed with PRAJA2 and PKAR2 antibodies, as well as subjected to Hoechst stain. PRAJA2 shows perinuclear localization, while PKAR2 is dispersed throughout the cell, with increased concentration at the plasma membrane (Figure 13). Co-localization of PRAJA2 and PKAR2 was not detected in this experiment basally or following stimulation.

3.11 Lentiviral production and infection of primary human differentiated adipocytes.

Attempts were made to test the effects of reducing PRAJA2 expression (knockdown) on lipolytic activity following stimulation of the differentiated adipocytes. Our laboratory has previously been successful with inducible shRNA lentiviral knockdown (of PDGFR-β) in primary human preadipocytes. However, this procedure had not been attempted on differentiated adipocytes. HEK293FT were transfected (~25-50%) to produce lentivirus, containing shRNA against PDGFR-β (Figure 14A). This virus was the applied to primary

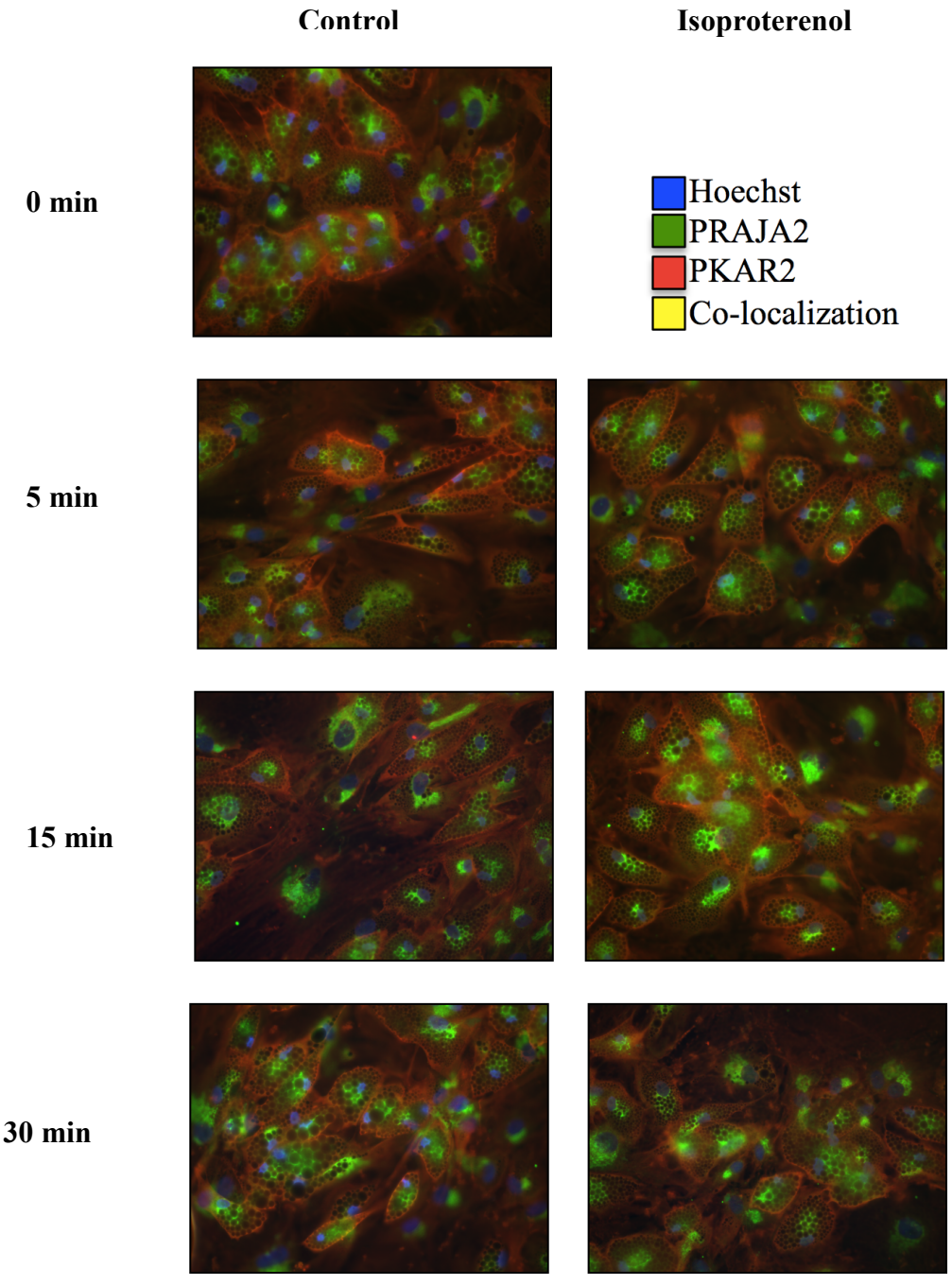
Control
Isoproterenol
0 min
5 min
15 min
30 min
Hoechst
PRAJA2
PKAR2
Co-localization

Figure 13. ***PRAJA2 and PKAR2 localization analysis, shown via immunohistochemistry.*** Human primary differentiated adipocytes were treated with 1μM isoproterenol or vehicle for 0, 5, 15 or 30mins. Cellular lysates were fixed and subject to double immunostaining with anti-PRAJA2 (Rb-Alexa Fluor 488) and anti-PKAR2 (Mo-Cy3) antibodies, and stained with Hoechst. Images were collected and analyzed by fluorescent microscopy. Data from 3 separate patient samples were assessed, figure shows representative images.

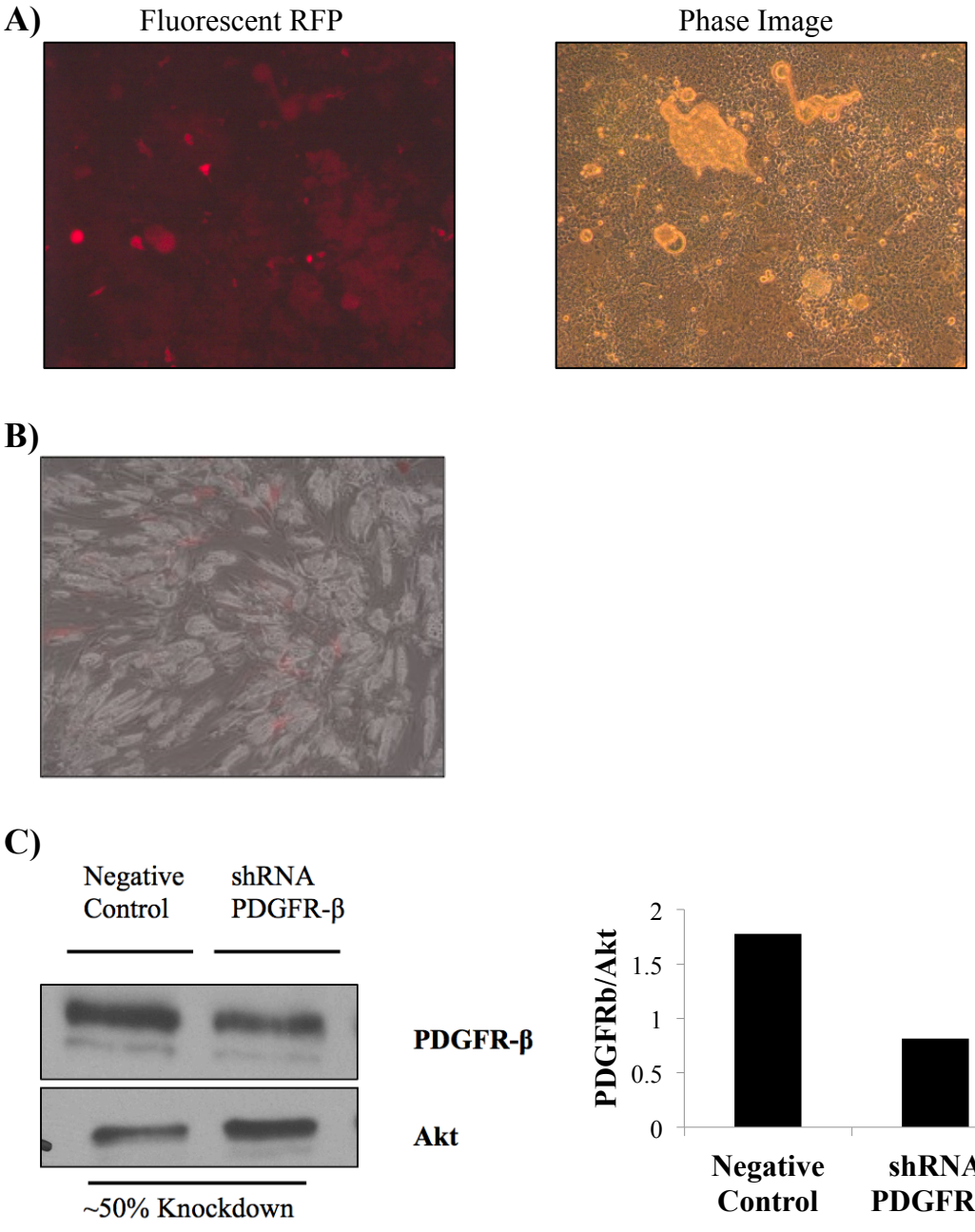
A)
Fluorescent RFP
Phase Image
B)
C)
Negative Control
shRNA PDGFR-β
PDGFR-β
Akt
~50% Knockdown
PDGFRb/Akt
2
1.5
1
0.5
0
Negative Control
shRNA PDGFR-β

Figure 14. ***Lentiviral production and infection of human primary differentiated adipocytes with PDGFR-β.*** HEK293FT cells were transfected with lentiviral packaging vectors psPAX2 and PMD2.G along with pTRIPZ vector containing shRNA targeting PDGFR-β **(A)**. Virus was collected in media of HEK293FT cells and applied for infection of primary human differentiated adipocytes, merged image shown **(B)**. Cellular proteins were separated by SDS-PAGE and immunoblotted for PDGFR-β and Akt (loading control) (n=1) **(C)**. Doxycycline induced RFP expression from the pTRIPZ vector was used to assess transfection and infection efficiency.

human differentiated adipocytes to infect them, with ~40% infection rate (Figure 14B), and achieving ~50% knockdown, as determined via immunoblot analysis (Figure 14C).

Next, shRNA targeted to PRAJA2 was used to assess the effect this would have on the lipolytic response of differentiated adipocytes stimulated with TSH or isoproterenol. HEK293FT were transfected (~25%), as assessed by analysis of doxycycline induced RFP signal (Figure 15). However, no infection of the differentiated adipocytes was identified after application with the lentivirus (n=2).

Fluorescent RFP

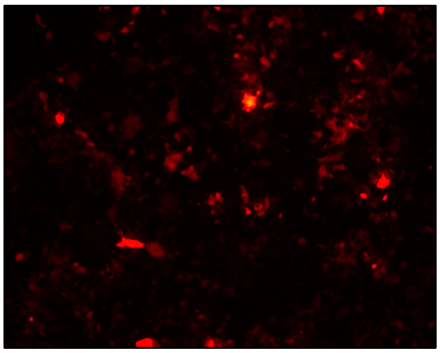

Phase Image

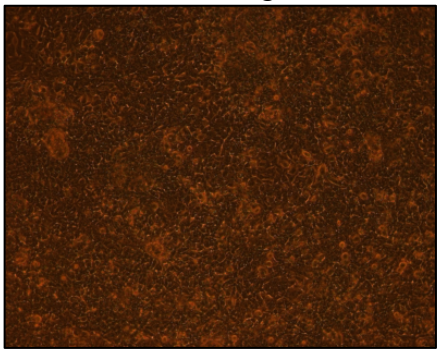

Figure 15. ***Lentiviral production containing PRAJA2 shRNA.*** HEK293FT cells were transfected with lentiviral packaging vectors psPAX2 and PMD2.G along with pTRIPZ vector containing shRNA targeting PRAJA2 **(A)**. Transfection of HEK293FT cells was performed with pTRIPZ vector containing shRNA targeting PRAJA2. Doxycycline induced RFP expression from the pTRIPZ vector was used to assess transfection efficiency.

4. DISCUSSION

4.1 Dysregulation of lipolysis in disease states and potential regulatory role of PRAJA2 in lipolysis

Lipolysis is an important metabolic pathway for mobilizing lipids from adipocytes in times of energy need. However, various disease states such as obesity-associated insulin resistance and SCH have been associated with excessive lipolysis. Dysregulation of this pathway disturbs energy homeostasis and results in increases in plasma NEFA and glycerol (Reynisdottir et al., 1994). These lipolytic byproducts are shuttled to other tissues through the blood stream, with the potential of disrupting their function. This metabolic dysfunction has been linked to pathophysiological states such as T2D and CVD (Arner, 2005).

PRAJA2 has recently been identified as a novel AKAP and E3 ubiquitin ligase that acts on regulatory units of various kinases. PRAJA2 has been termed a cancer-related gene showing importance in signaling pathways, which promote malignant transformation, tumor growth and cell survival (Cantara et al., 2012; Hedrick et al., 2013; Lignitto et al., 2013). Important to this thesis, PRAJA2 has been reported to act on PKAR2 in the context of long-term memory storage, and shows increased expression in thyroid cancer cells that are dependent on PKA (Cantara et al., 2012; Lignitto et al., 2011).

Given these features of PRAJA2 activity, it was hypothesized it might be important in regulating the GPCR-stimulated, PKA-mediated, lipolytic pathway in adipocytes (Lafontan and Langin, 2009). PRAJA2, in the presence of high intracellular cAMP, has been described to target PKAR for ubiquitination, subsequently resulting in its degradation by the proteasome. This reduction in PKAR prolongs cellular PKAC activity (Lignitto et al., 2011). In the context of lipolysis, this would mean prolonged lipolytic signaling in the presence of

PRAJA2 activity, ultimately resulting in increased release of NEFA and glycerol from adipocytes. Conversely, in the absence of PRAJA2 activity, adipocytes would display blunted lipolysis, with an abundance of PKAR readily available to re-associate with PKAC, terminating the signal.

PRAJA2, a novel AKAP/E3 ubiquitin ligase, was studied in human primary differentiated adipocytes to learn how it might affect PKA signaling and lipolysis. PRAJA2 expression, phosphorylation, protein-protein interactions and cellular localization were investigated under basal and TSH- or isoproterenol-stimulated conditions. The results demonstrated that stimulation with TSH or isoproterenol does not change PRAJA2 mRNA or protein expression levels in adipocytes. These data suggest the phosphorylation state of PRAJA2 and PRAJA2-dependent protein-protein interactions may be affected by isoproterenol, but not TSH. Cellular localization of PRAJA2 was unaffected by agonist stimulation.

4.2 TSH and isoproterenol stimulate lipolysis in primary human differentiated adipocytes

First, it was demonstrated that TSH or isoproterenol stimulates lipolysis in human primary differentiated adipocytes, as previously shown by our research group (Gagnon et al., 2010). These data show up to a 3-fold increase in NEFA and a 7-fold in glycerol release upon TSH/isoproterenol stimulation when compared to basal condition. Isoproterenol, as a well-documented $\beta_{1,2}$-AR agonist, strongly stimulates lipolysis in human adipocytes (Lafontan and Langin, 2009). More recently, human adipocytes have been shown to express TSHR and are described as a novel extra-thyroidal TSH target (Davies et al., 2002; Sorisky

et al., 2000). This TSH stimulation initiates a PKA-dependent signal cascade, resulting in increases in plasma NEFA and glycerol (Gagnon et al., 2010).

Patients with SCH have increased plasma NEFA and glycerol levels, suggesting increased lipolysis (Caraccio et al., 2005). SCH is characterized by TSH levels >5mU/L with normal thyroid hormone levels (Surks and Ocampo, 1996). In this study 5mU/mL and 50mU/mL TSH is used to stimulate human differentiated adipocytes. These levels are supraphysiological by 1000-fold when compared to the SCH state. However, in vitro studies on thyrocytes, the established physiological target of TSH, also require these high levels (Back et al., 2013; Brewer et al., 2007). This suggests that the *in vitro* sensitivity to TSH is lower, although the reasons for this remain unclear.

4.3 Characterization of the expression of PRAJA2 in primary human differentiated adipocytes

PRAJA2 expression in human primary preadipocytes and differentiated adipocytes was investigated. These data shows that PRAJA2 is expressed equally in preadipocytes and differentiated adipocytes at the protein level. Additionally, It was shown that expression of PRAJA2 mRNA and protein, in differentiated adipocytes, did not significantly change upon TSH or isoproterenol stimulation for up to 24 and 48 hours respectively. This establishes that PRAJA2 is expressed in adipocytes, affirming its potential importance in this cellular system.

4.4 Investigation of PRAJA2 phosphorylation and protein-protein interactions in primary human differentiated adipocytes

Little is known about how PRAJA2 functions as a regulator of cellular signaling events. Lignitto *et al*. have best described the functional role of PRAJA2 in PKA regulation.

They report PRAJA2 as a PKAC phosphorylation target, which activates its E3 ubiquitin ligase towards its substrate, PKAR (Lignitto et al., 2011). This results in degradation of PKAR and prolonging of PKAC action. This could be predicted to augment lipolysis in adipocytes, by increasing PKA-dependent phosphorylation of perilipin and HSL (Lafontan and Langin, 2009).

The phosphorylation state of PRAJA2 action is shown to activate its catalytic E3 ubiquitin ligase activity (Lignitto et al., 2011). To investigate if endogenous PRAJA2 is phosphorylated by PKA in adipocytes, PRAJA2 immunoprecipitation studies were performed on differentiated adipocytes under basal and stimulated conditions. The immunoprecipitates were analyzed for PKA substrates that were phosphorylated at the consensus sequence RRXS*/T* (Kemp et al., 1977). These data reveal 122kDa and 69kDa proteins which co-immunoprecipitate with PRAJA2 and are phosphorylated by PKA; this phosphorylation is increased in response to isoproterenol, but not TSH stimulation.

The phosphorylated PKA substrate of approximately 122kDa may be PRAJA2, detected at ~120kDa via immunoblot. Alternatively the protein detected may be a PRAJA2-associated protein migrating at a similar position, which is phosphorylated by PKA. Further investigations of SDS-PAGE, band excision and analysis by mass spectrometry are required to identify this protein.

Confirmation experiments were attempted for the results seen in the PRAJA2 immunoprecipitation by performing a pPKAsub immunoprecipitation and analyzing the immunoprecipitates for PRAJA2. This would potentially identify the 122kDa band as phosphorylated PRAJA2. However, this experiment did not identify PRAJA2 in the immunoprecipitate under basal or stimulated conditions. This may be due to antibody specificity, availability of the phosphorylation site for antibody binding and/or relative

concentration of the various PKA substrates in the lysate. Alternatively, the 122kDa band may simply be a PRAJA2-associated protein and therefore would not be detected with the PRAJA2 antibody.

As stated, PRAJA2 immunoprecipitation experiments allowed the assessment of PRAJA2-associated proteins. These data show a phosphorylated PKA substrate of approximately 69kDa in my differentiated adipocytes. The phosphorylation of this 69kDa protein was significantly increased following a 15-minute stimulation with isoproterenol, when compared to the basal condition. Stimulation with TSH did not significantly increase the amount of phosphorylated protein detected. It is unknown, which, if any proteins of the lipolytic pathway interact with PRAJA2. The main PKA phosphorylation targets important for lipolytic pathway are perilipin and HSL, which are detectable at 81/83kDa and 62kDa respectively via immunoblot (Krawczyk et al., 2012). These proteins, although PKA targets, do not correspond to the molecular weight of this band of interest, 69kDa. This suggests PRAJA2 does not interact with HSL and perilipin and that further analysis, through mass spectrometry, is required to identify the protein(s).

A higher dose of TSH (50mU/mL, as opposed to 5mU/mL) should be tested before excluding TSH as a regulator of PRAJA2 regulation. This higher dose has shown similar potency to isoproterenol stimulation, as seen in the lipolysis experiments presented. Alternatively, it is possible that there are qualitative differences in isoproterenol and TSH signaling (Lafontan and Langin, 2009; Thrush et al., 2012). Future studies could include mass spectrometry analysis of these bands to identify these protein(s).

Additional immunoprecipitation experiments were performed to assess interactions between PKAR2 and PRAJA2, as described in other cell systems (Hedrick et al., 2013; Lignitto et al., 2011). However, PRAJA2 was not detected in the PKAR2

immunoprecipitates. Due to the experimental design using endogenously expressed proteins in primary cells, and my inability to assess the performance of this immunoprecipitation, This association should not yet be discounted in primary differentiated adipocytes. In future studies, increasing and concentrating the sample, overexpressing PRAJA2 and/or utilizing a different commercially available method of removing the antibody IgG from the sample for post-analysis, may better assess whether this association occurs in this cellular model. Additionally, it is possible that this association is weak, or hinders the PKAR2 antibody-binding site, making this experimental approach ill suited to assess this interaction.

4.5 Analysis of localization and AKAP function of PRAJA2

To further characterize PRAJA2 in adipocytes, immunohistochemistry of PRAJA2 and PKAR2 was performed under basal conditions and following isoproterenol stimulation to assess localization. Lignitto *et al*., (2011) show partial co-localization of PRAJA2 and PKAR2, supporting their interaction and PRAJA2's AKAP function (Lignitto et al., 2011). Following the current model, under basal conditions PRAJA2 and PKAR2 would show co-localization at the plasma membrane, which would dissipate following stimulation, due to the activation of PRAKA2's E3 ligase activity and proteasomal degradation of PKAR2. These data show perinuclear localization of PRAJA2, whereas PKAR2 localizes to the plasma membrane, no co-localization is seen at this magnification. Additionally, no change in localization was apparent following cellular stimulation with isoproterenol.

More sophisticated microscopy techniques, such as confocal microscopy, may allow better resolution for analysis of this possible association. Due to the 3-dimentional nature of differentiated adipocytes, they can be difficult to assess using single-plane fluorescence microscopy. However, it is also possible that PKAR2 is simply not a target for PRAJA2

AKAP or E3 ubiquitin ligase activity in this cellular model and that PRAJA2 does not play a role in the TSH/isoproterenol stimulated, PKA-mediated lipolytic pathway.

4.6 Determining the effect of down-regulating PRAJA2 expression on TSH- and isoproterenol-stimulated lipolysis in primary human differentiated adipocytes

It was hypothesized that knockdown of PRAJA2 would lead to blunted lipolysis. PKAR would see a reduction in ubiquitination and degradation and would therefore be available for re-attachment to PKAC, terminating its kinase activity within the cell. The plan was to measure NEFA and glycerol levels in the cellular media following lentiviral shRNA knockdown of PRAJA2 in both stimulated and basal conditions.

Following successful transfection of HEK293, lentivirus targeting PDGFR-β for knockdown was collected. Subsequently, differentiated adipocytes were infected achieving ~50% knockdown of the target gene, as analyzed by immunoblot. Unfortunately, following production of lentivirus targeting PRAJA2, infection and knockdown of PRAJA2, using the same approach was not successful. Future studies should try another method of delivery, such as siRNA particles. Alternatively, this investigation could be applied to mouse 3T3-L1 differentiated adipocytes, which are easier to manipulate, in terms of gene expression; however, regulation of PRAJA2 could be different in this mouse cell line, as compared to human differentiated adipocytes. Future studies could also address the effects of overexpressing PRAJA2 on lipolytic response of differentiated adipocytes. Overexpression would be predicted to enhance lipolytic signaling via increasing the ubiquitination and proteasomal degradation of PKAR, prolonging PKAC activity, ultimately resulting in increased NEFA and glycerol release. PRAJA2 could then potentially be further studied in

its contribution as a risk factor for T2D, CVD and other aspects of metabolic syndrome (Arner, 2005).

4.7 Proposed Model

A model of PRAJA2 action in GPCR-stimulated PKA-medicated pathways has previously been proposed (Figure 1) (Lignitto et al., 2011). Here, PRAJA2 is shown to be equally expressed in human preadipocyte and differentiated adipocytes. The expression of this protein in differentiated adipocytes show no change at the mRNA or protein levels upon stimulation with TSH or isoproterenol. Stimulation with isoproterenol leads to an increase in PKA-mediated phosphorylation of a 122kDa protein and a 69kDa protein, which interact with PRAJA2. Association between PRAJA2 and PKAR was not observed; however, further experimentation is required before discounting this interaction. In addition, PRAJA2 targets other proteins in different cellular models and may have an operative role in another signaling pathway in these cells.

5. CONCLUSION

In summation, this thesis provides insight into the potential role of PRAJA2 in the regulation of TSH- or isoproterenol- stimulated, PKA-mediated lipolysis. Specifically, It is shown here, for the first time, that PRAJA2 is expressed equally in primary human preadipocytes and differentiated adipocytes. Its expression at the mRNA and protein levels does not change following TSH or isoproterenol stimulation. Additionally, PRAJA2 is shown to interact with other cellular proteins, which are PKA phosphorylation targets. Following stimulation with isoproterenol, but not TSH at the concentrations presented, these proteins show increased phosphorylation; however, more work is needed in order to confirm the identities of these proteins. Confirmation of interaction and co-localization between PRAJA2 and PKAR2, as previously suggested by literature; was not successful, nevertheless further investigations in this cellular model should be pursued. Taken together, these results indicate the presence and potential for PRAJA2 involvement in regulating lipolytic, or other TSH/isoproterenol-stimulated, PKA-mediated signaling pathways in this cellular model.

6. FUTURE WORK

Given the described results, further research is needed to determine the role of PRAJA2 activity in differentiated adipocytes. The current findings reveal two proteins (122kDa and 69kDa), which interact with PRAJA2 and are phosphorylated in a PKA-dependent manner upon GPCR stimulation. These signals suggest that PRAJA2 may have key interactions and is playing some role in a PKA-mediated pathway, however the proteins' identities remain unknown. Hence, to determine the identities of these proteins, mass spectrometry on SDS-PAGE excised bands should be pursued. Further work is also needed to clarify if there is an interaction and possible co-localization of PRAJA2 and PKAR2. Finally, additional work on analyzing the effects of PRAJA2 knockdown in lipolysis should be considered, such as the use of siRNA particles. More research is needed to elucidate the potential role of PRAJA2 in hormone-stimulated lipolysis or other TSH/isoproterenol-stimulated, PKA-mediated pathways in differentiated adipocytes.

7. REFERENCES

Anthonsen, M.W., Ronnstrand, L., Wernstedt, C., Degerman, E., and Holm, C. (1998). Identification of novel phosphorylation sites in hormone-sensitive lipase that are phosphorylated in response to isoproterenol and govern activation properties in vitro. J. Biol. Chem. *273,* 215-221.

Antunes, T.T., Gagnon, A., Langille, M.L., and Sorisky, A. (2008). Thyroid-stimulating hormone induces interleukin-6 release from human adipocytes through activation of the nuclear factor-kappaB pathway. Endocrinology *149,* 3062-3066.

Ardley, H.C., and Robinson, P.A. (2005). E3 ubiquitin ligases. Essays Biochem. *41,* 15-30.

Arner, P. (2005). Human fat cell lipolysis: biochemistry, regulation and clinical role. Best Pract. Res. Clin. Endocrinol. Metab. *19,* 471-482.

Arner, P. (1988). Control of lipolysis and its relevance to development of obesity in man. Diabetes Metab. Rev. *4,* 507-515.

Arner, P., and Spalding, K.L. (2010). Fat cell turnover in humans. Biochem. Biophys. Res. Commun. *396,* 101-104.

Azuma, K., Heilbronn, L.K., Albu, J.B., Smith, S.R., Ravussin, E., Kelley, D.E., and Look AHEAD Adipose Research Group. (2007). Adipose tissue distribution in relation to insulin resistance in type 2 diabetes mellitus. Am. J. Physiol. Endocrinol. Metab. *293,* E435-42.

Back, C.M., Stohr, S., Schafer, E.A., Biebermann, H., Boekhoff, I., Breit, A., Gudermann, T., and Buch, T.R. (2013). TSH induces metallothionein 1 in thyrocytes via Gq/11- and PKC-dependent signaling. J. Mol. Endocrinol. *51,* 79-90.

Barbe, P., Millet, L., Galitzky, J., Lafontan, M., and Berlan, M. (1996). In situ assessment of the role of the beta 1-, beta 2- and beta 3-adrenoceptors in the control of lipolysis and nutritive blood flow in human subcutaneous adipose tissue. Br. J. Pharmacol. *117,* 907-913.

Blaak, E.E. (2000). Adrenergically stimulated fat utilization and ageing. Ann. Med. *32,* 380-382.

Boelen, A., Kwakkel, J., and Fliers, E. (2012). Thyroid hormone receptors in health and disease. Minerva Endocrinol. *37,* 291-304.

Bolinder, J., Lindblad, A., Engfeldt, P., and Arner, P. (1987). Studies of acute effects of insulin-like growth factors I and II in human fat cells. J. Clin. Endocrinol. Metab. *65,* 732-737.

Boston, B.A. (1999). The role of melanocortins in adipocyte function. Ann. N. Y. Acad. Sci. *885,* 75-84.

Brasaemle, D.L. (2007). Thematic review series: adipocyte biology. The perilipin family of structural lipid droplet proteins: stabilization of lipid droplets and control of lipolysis. J. Lipid Res. *48,* 2547-2559.

Brasaemle, D.L., Subramanian, V., Garcia, A., Marcinkiewicz, A., and Rothenberg, A. (2009). Perilipin A and the control of triacylglycerol metabolism. Mol. Cell. Biochem. *326,* 15-21.

Brewer, C., Yeager, N., and Di Cristofano, A. (2007). Thyroid-stimulating hormone initiated proliferative signals converge in vivo on the mTOR kinase without activating AKT. Cancer Res. *67,* 8002-8006.

Cai, T.Q., Ren, N., Jin, L., Cheng, K., Kash, S., Chen, R., Wright, S.D., Taggart, A.K., and Waters, M.G. (2008). Role of GPR81 in lactate-mediated reduction of adipose lipolysis. Biochem. Biophys. Res. Commun. *377,* 987-991.

Cantara, S., D'Angeli, F., Toti, P., Lignitto, L., Castagna, M.G., Capuano, S., Prabhakar, B.S., Feliciello, A., and Pacini, F. (2012). Expression of the ring ligase PRAJA2 in thyroid cancer. J. Clin. Endocrinol. Metab. *97,* 4253-4259.

Caraccio, N., Natali, A., Sironi, A., Baldi, S., Frascerra, S., Dardano, A., Monzani, F., and Ferrannini, E. (2005). Muscle metabolism and exercise tolerance in subclinical hypothyroidism: a controlled trial of levothyroxine. J. Clin. Endocrinol. Metab. *90,* 4057-4062.

Carmen, G.Y., and Victor, S.M. (2006). Signalling mechanisms regulating lipolysis. Cell. Signal. *18,* 401-408.

Chain, D.G., Schwartz, J.H., and Hegde, A.N. (1999). Ubiquitin-mediated proteolysis in learning and memory. Mol. Neurobiol. *20,* 125-142.

Choi, Y.H., Park, S., Hockman, S., Zmuda-Trzebiatowska, E., Svennelid, F., Haluzik, M., Gavrilova, O., Ahmad, F., Pepin, L., Napolitano, M.*, et al.* (2006). Alterations in regulation of energy homeostasis in cyclic nucleotide phosphodiesterase 3B-null mice. J. Clin. Invest. *116,* 3240-3251.

Chowdhury, S., Howell, G.M., Rajput, A., Teggart, C.A., Brattain, L.E., Weber, H.R., Chowdhury, A., and Brattain, M.G. (2011). Identification of a novel TGFbeta/PKA signaling transduceome in mediating control of cell survival and metastasis in colon cancer. PLoS One *6,* e19335.

Ciechanover, A., Elias, S., Heller, H., and Hershko, A. (1982). "Covalent affinity" purification of ubiquitin-activating enzyme. J. Biol. Chem. *257,* 2537-2542.

Cinti, S., Mitchell, G., Barbatelli, G., Murano, I., Ceresi, E., Faloia, E., Wang, S., Fortier, M., Greenberg, A.S., and Obin, M.S. (2005). Adipocyte death defines macrophage localization and function in adipose tissue of obese mice and humans. J. Lipid Res. *46,* 2347-2355.

Coppack, S.W., Jensen, M.D., and Miles, J.M. (1994). In vivo regulation of lipolysis in humans. J. Lipid Res. *35,* 177-193.

Cornelius, P., MacDougald, O.A., and Lane, M.D. (1994). Regulation of adipocyte development. Annu. Rev. Nutr. *14,* 99-129.

Cristancho, A., and Lazar, M. (2011). Forming functional fat: a growing understanding of adipocyte differentiation. Nat. Rev. Mol. Cell. Biol. *12*, 722-734.

Danforth, E.,Jr. (2000). Failure of adipocyte differentiation causes type II diabetes mellitus? Nat. Genet. *26,* 13.

Davies, T., Marians, R., and Latif, R. (2002). The TSH receptor reveals itself. J. Clin. Invest. *110,* 161-164.

Fain, J.N., Madan, A.K., Hiler, M.L., Cheema, P., and Bahouth, S.W. (2004). Comparison of the release of adipokines by adipose tissue, adipose tissue matrix, and adipocytes from visceral and subcutaneous abdominal adipose tissues of obese humans. Endocrinology *145,* 2273-2282.

Fedorenko, A., Lishko, P.V., and Kirichok, Y. (2012). Mechanism of fatty-acid-dependent UCP1 uncoupling in brown fat mitochondria. Cell *151,* 400-413.

Fox, C.S., Massaro, J.M., Hoffmann, U., Pou, K.M., Maurovich-Horvat, P., Liu, C.Y., Vasan, R.S., Murabito, J.M., Meigs, J.B., Cupples, L.A., D'Agostino RB, S., and O'Donnell, C.J. (2007). Abdominal visceral and subcutaneous adipose tissue compartments: association with metabolic risk factors in the Framingham Heart Study. Circulation *116,* 39-48.

Fredrikson, G., Tornqvist, H., and Belfrage, P. (1986). Hormone-sensitive lipase and monoacylglycerol lipase are both required for complete degradation of adipocyte triacylglycerol. Biochim. Biophys. Acta *876,* 288-293.

Gagnon, A., Antunes, T.T., Ly, T., Pongsuwan, P., Gavin, C., Lochnan, H.A., and Sorisky, A. (2010). Thyroid-stimulating hormone stimulates lipolysis in adipocytes in culture and raises serum free fatty acid levels in vivo. Metabolism *59,* 547-553.

Gagnon, A., Foster, C., Landry, A., and Sorisky, A. (2013). The role of interleukin 1beta in the anti-adipogenic action of macrophages on human preadipocytes. J. Endocrinol. *217,* 197-206.

Galitzky, J., Langin, D., Verwaerde, P., Montastruc, J.L., Lafontan, M., and Berlan, M. (1997). Lipolytic effects of conventional beta 3-adrenoceptor agonists and of CGP 12,177 in

rat and human fat cells: preliminary pharmacological evidence for a putative beta 4-adrenoceptor. Br. J. Pharmacol. *122,* 1244-1250.

Garten, A., Schuster, S., and Kiess, W. (2012). The insulin-like growth factors in adipogenesis and obesity. Endocrinol. Metab. Clin. North Am. *41,* 283-95, v-vi.

Green, H., and Meuth, M. (1974). An established pre-adipose cell line and its differentiation in culture. Cell *3,* 127-133.

Greenberg, A.S., Egan, J.J., Wek, S.A., Moos, M.C.,Jr, Londos, C., and Kimmel, A.R. (1993). Isolation of cDNAs for perilipins A and B: sequence and expression of lipid droplet-associated proteins of adipocytes. Proc. Natl. Acad. Sci. U. S. A. *90,* 12035-12039.

Gregoire, F.M. (2001). Adipocyte differentiation: from fibroblast to endocrine cell. Exp. Biol. Med. (Maywood) *226,* 997-1002.

Guilherme, A., Virbasius, J.V., Puri, V., and Czech, M.P. (2008). Adipocyte dysfunctions linking obesity to insulin resistance and type 2 diabetes. Nat. Rev. Mol. Cell Biol. *9,* 367-377.

Haemmerle, G., Lass, A., Zimmermann, R., Gorkiewicz, G., Meyer, C., Rozman, J., Heldmaier, G., Maier, R., Theussl, C., Eder, S.*, et al.* (2006). Defective lipolysis and altered energy metabolism in mice lacking adipose triglyceride lipase. Science *312,* 734-737.

Hauner, H. (2005). Secretory factors from human adipose tissue and their functional role. Proc. Nutr. Soc. *64,* 163-169.

Hauner, H., Skurk, T., and Wabitsch, M. (2001). Cultures of human adipose precursor cells. Methods Mol. Biol. *155,* 239-247.

Hedrick, E.D., Agarwal, E., Leiphrakpam, P.D., Haferbier, K.L., Brattain, M.G., and Chowdhury, S. (2013). Differential PKA activation and AKAP association determines cell fate in cancer cells. J. Mol. Signal. *8,* 10-2187-8-10.

Hergovich, A. (2011). MOB control: reviewing a conserved family of kinase regulators. Cell. Signal. *23,* 1433-1440.

Hibuse, T., Maeda, N., Nagasawa, A., and Funahashi, T. (2006). Aquaporins and glycerol metabolism. Biochim. Biophys. Acta *1758,* 1004-1011.

Holm, C. (2003). Molecular mechanisms regulating hormone-sensitive lipase and lipolysis. Biochem. Soc. Trans. *31,* 1120-1124.

Horowitz, J.F., and Klein, S. (2000). Lipid metabolism during endurance exercise. Am. J. Clin. Nutr. *72,* 558S-63S.

Janson, A., Rawet, H., Perbeck, L., and Marcus, C. (1998). Presence of thyrotropin receptor in infant adipocytes. Pediatr. Res. *43,* 555-558.

Karlsson, M., Contreras, J.A., Hellman, U., Tornqvist, H., and Holm, C. (1997). cDNA cloning, tissue distribution, and identification of the catalytic triad of monoglyceride lipase. Evolutionary relationship to esterases, lysophospholipases, and haloperoxidases. J. Biol. Chem. *272,* 27218-27223.

Kemp, B.E., Graves, D.J., Benjamini, E., and Krebs, E.G. (1977). Role of multiple basic residues in determining the substrate specificity of cyclic AMP-dependent protein kinase. J. Biol. Chem. *252,* 4888-4894.

Kershaw, E.E., Hamm, J.K., Verhagen, L.A., Peroni, O., Katic, M., and Flier, J.S. (2006). Adipose triglyceride lipase: function, regulation by insulin, and comparison with adiponutrin. Diabetes *55,* 148-157.

Kim, K.H., Lee, K., Moon, Y.S., and Sul, H.S. (2001). A cysteine-rich adipose tissue-specific secretory factor inhibits adipocyte differentiation. J. Biol. Chem. *276,* 11252-11256.

Kishida, K., Kuriyama, H., Funahashi, T., Shimomura, I., Kihara, S., Ouchi, N., Nishida, M., Nishizawa, H., Matsuda, M., Takahashi, M*., et al.* (2000). Aquaporin adipose, a putative glycerol channel in adipocytes. J. Biol. Chem. *275,* 20896-20902.

Kraemer, F.B., and Shen, W.J. (2002). Hormone-sensitive lipase: control of intracellular tri-(di-)acylglycerol and cholesteryl ester hydrolysis. J. Lipid Res. *43,* 1585-1594.

Krawczyk, S.A., Haller, J.F., Ferrante, T., Zoeller, R.A., and Corkey, B.E. (2012). Reactive oxygen species facilitate translocation of hormone sensitive lipase to the lipid droplet during lipolysis in human differentiated adipocytes. PLoS One *7,* e34904.

Lafontan, M. (2014). Adipose tissue and adipocyte dysregulation. Diabetes Metab. *40,* 16-28.

Lafontan, M., and Agid, R. (1979). An extra-adrenal action of adrenocorticotrophin: physiological induction of lipolysis by secretion of adrenocorticotrophin in obese rabbits. J. Endocrinol. *81,* 281-290.

Lafontan, M., and Berlan, M. (1995). Fat cell alpha 2-adrenoceptors: the regulation of fat cell function and lipolysis. Endocr. Rev. *16,* 716-738.

Lafontan, M., and Langin, D. (2009). Lipolysis and lipid mobilization in human adipose tissue. Prog. Lipid Res. *48,* 275-297.

Lagerstrom, M.C., and Schioth, H.B. (2008). Structural diversity of G protein-coupled receptors and significance for drug discovery. Nat. Rev. Drug Discov. *7,* 339-357.

LaLonde, J.M., Bernlohr, D.A., and Banaszak, L.J. (1994). The up-and-down beta-barrel proteins. FASEB J. *8,* 1240-1247.

Lass, A., Zimmermann, R., Haemmerle, G., Riederer, M., Schoiswohl, G., Schweiger, M., Kienesberger, P., Strauss, J.G., Gorkiewicz, G., and Zechner, R. (2006). Adipose triglyceride lipase-mediated lipolysis of cellular fat stores is activated by CGI-58 and defective in Chanarin-Dorfman Syndrome. Cell. Metab. *3,* 309-319.

Lee, M.J., Wu, Y., and Fried, S.K. (2013). Adipose tissue heterogeneity: implication of depot differences in adipose tissue for obesity complications. Mol. Aspects Med. *34,* 1-11.

Leinninger, G.M., Jo, Y.H., Leshan, R.L., Louis, G.W., Yang, H., Barrera, J.G., Wilson, H., Opland, D.M., Faouzi, M.A., Gong, Y.*, et al.* (2009). Leptin acts via leptin receptor-expressing lateral hypothalamic neurons to modulate the mesolimbic dopamine system and suppress feeding. Cell. Metab. *10,* 89-98.

Lignitto, L., Arcella, A., Sepe, M., Rinaldi, L., Delle Donne, R., Gallo, A., Stefan, E., Bachmann, V.A., Oliva, M.A., Tiziana Storlazzi, C.*, et al.* (2013). Proteolysis of MOB1 by the ubiquitin ligase praja2 attenuates Hippo signalling and supports glioblastoma growth. Nat. Commun. *4,* 1822.

Lignitto, L., Carlucci, A., Sepe, M., Stefan, E., Cuomo, O., Nistico, R., Scorziello, A., Savoia, C., Garbi, C., Annunziato, L., and Feliciello, A. (2011). Control of PKA stability and signalling by the RING ligase praja2. Nat. Cell Biol. *13,* 412-422.

Lignitto, L., Sepe, M., Carlucci, A., and Feliciello, A. (2011). An intimate connection between ubiquitination and compartmentalized cAMP signaling. Cell. Cycle *10,* 2051-2052.

Liu, C., Wu, J., Zhu, J., Kuei, C., Yu, J., Shelton, J., Sutton, S.W., Li, X., Yun, S.J., Mirzadegan, T.*, et al.* (2009). Lactate inhibits lipolysis in fat cells through activation of an orphan G-protein-coupled receptor, GPR81. J. Biol. Chem. *284,* 2811-2822.

Maratou, E., Hadjidakis, D.J., Kollias, A., Tsegka, K., Peppa, M., Alevizaki, M., Mitrou, P., Lambadiari, V., Boutati, E., Nikzas, D.*, et al.* (2009). Studies of insulin resistance in patients with clinical and subclinical hypothyroidism. Eur. J. Endocrinol. *160,* 785-790.

Marcus, C., Ehren, H., Bolme, P., and Arner, P. (1988). Regulation of lipolysis during the neonatal period. Importance of thyrotropin. J. Clin. Invest. *82,* 1793-1797.

Matarese, V., and Bernlohr, D.A. (1988). Purification of murine adipocyte lipid-binding protein. Characterization as a fatty acid- and retinoic acid-binding protein. J. Biol. Chem. *263,* 14544-14551.

Mauriege, P., De Pergola, G., Berlan, M., and Lafontan, M. (1988). Human fat cell beta-adrenergic receptors: beta-agonist-dependent lipolytic responses and characterization of beta-

adrenergic binding sites on human fat cell membranes with highly selective beta 1-antagonists. J. Lipid Res. *29,* 587-601.

Mercader, J., Wanecq, E., Chen, J., and Carpene, C. (2011). Isopropylnorsynephrine is a stronger lipolytic agent in human adipocytes than synephrine and other amines present in Citrus aurantium. J. Physiol. Biochem. *67,* 443-452.

Mishra, L., Tully, R.E., Monga, S.P., Yu, P., Cai, T., Makalowski, W., Mezey, E., Pavan, W.J., and Mishra, B. (1997). Praja1, a novel gene encoding a RING-H2 motif in mouse development. Oncogene *15,* 2361-2368.

Obeyesekere, M.N., Klein, G.J., Nattel, S., Leong-Sit, P., Gula, L.J., Skanes, A.C., Yee, R., and Krahn, A.D. (2013). A clinical approach to early repolarization. Circulation *127,* 1620-1629.

Ouchi, N., Parker, J.L., Lugus, J.J., and Walsh, K. (2011). Adipokines in inflammation and metabolic disease. Nat. Rev. Immunol. *11,* 85-97.

Pagnon, J., Matzaris, M., Stark, R., Meex, R.C., Macaulay, S.L., Brown, W., O'Brien, P.E., Tiganis, T., and Watt, M.J. (2012). Identification and functional characterization of protein kinase A phosphorylation sites in the major lipolytic protein, adipose triglyceride lipase. Endocrinology *153,* 4278-4289.

Park, B.O., Ahrends, R., and Teruel, M.N. (2012). Consecutive positive feedback loops create a bistable switch that controls preadipocyte-to-adipocyte conversion. Cell. Rep. *2,* 976-990.

Pasarica, M., Sereda, O.R., Redman, L.M., Albarado, D.C., Hymel, D.T., Roan, L.E., Rood, J.C., Burk, D.H., and Smith, S.R. (2009). Reduced adipose tissue oxygenation in human obesity: evidence for rarefaction, macrophage chemotaxis, and inflammation without an angiogenic response. Diabetes *58,* 718-725.

Pidoux, G., and Tasken, K. (2010). Specificity and spatial dynamics of protein kinase A signaling organized by A-kinase-anchoring proteins. J. Mol. Endocrinol. *44,* 271-284.

Raclot, T., Langin, D., Lafontan, M., and Groscolas, R. (1997). Selective release of human adipocyte fatty acids according to molecular structure. Biochem. J. *324 (Pt 3),* 911-915.

Reynisdottir, S., Ellerfeldt, K., Wahrenberg, H., Lithell, H., and Arner, P. (1994). Multiple lipolysis defects in the insulin resistance (metabolic) syndrome. J. Clin. Invest. *93,* 2590-2599.

Richelsen, B. (1988). Prostaglandin E2 action and binding in human adipocytes: effects of sex, age, and obesity. Metabolism *37,* 268-275.

Robidoux, J., Martin, T.L., and Collins, S. (2004). Beta-adrenergic receptors and regulation of energy expenditure: a family affair. Annu. Rev. Pharmacol. Toxicol. *44,* 297-323.

Rodondi, N., den Elzen, W.P., Bauer, D.C., Cappola, A.R., Razvi, S., Walsh, J.P., Asvold, B.O., Iervasi, G., Imaizumi, M., Collet, T.H.*, et al.* (2010). Subclinical hypothyroidism and the risk of coronary heart disease and mortality. JAMA *304,* 1365-1374.

Rosen, E.D., Hsu, C.H., Wang, X., Sakai, S., Freeman, M.W., Gonzalez, F.J., and Spiegelman, B.M. (2002). C/EBPalpha induces adipogenesis through PPARgamma: a unified pathway. Genes Dev. *16,* 22-26.

Rosen, E.D., and Spiegelman, B.M. (2014). What we talk about when we talk about fat. Cell *156,* 20-44.

Sakamaki, J., Fu, A., Reeks, C., Baird, S., Depatie, C., Al Azzabi, M., Bardeesy, N., Gingras, A.C., Yee, S.P., and Screaton, R.A. (2014). Role of the SIK2-p35-PJA2 complex in pancreatic beta-cell functional compensation. Nat. Cell Biol. *16,* 234-244.

Saltiel, A.R., and Pessin, J.E. (2002). Insulin signaling pathways in time and space. Trends Cell Biol. *12,* 65-71.

Schweppe, R.E., Kerege, A.A., Sharma, V., Poczobutt, J.M., Gutierrez-Hartmann, A., Grzywa, R.L., and Haugen, B.R. (2009). Distinct genetic alterations in the mitogen-activated protein kinase pathway dictate sensitivity of thyroid cancer cells to mitogen-activated protein kinase kinase 1/2 inhibition. Thyroid *19,* 825-835.

Sengenes, C., Berlan, M., De Glisezinski, I., Lafontan, M., and Galitzky, J. (2000). Natriuretic peptides: a new lipolytic pathway in human adipocytes. FASEB J. *14,* 1345-1351.

Sengenes, C., Bouloumie, A., Hauner, H., Berlan, M., Busse, R., Lafontan, M., and Galitzky, J. (2003). Involvement of a cGMP-dependent pathway in the natriuretic peptide-mediated hormone-sensitive lipase phosphorylation in human adipocytes. J. Biol. Chem. *278,* 48617-48626.

Sengenes, C., Lolmede, K., Zakaroff-Girard, A., Busse, R., and Bouloumie, A. (2005). Preadipocytes in the human subcutaneous adipose tissue display distinct features from the adult mesenchymal and hematopoietic stem cells. J. Cell. Physiol. *205,* 114-122.

Sinha, T.K., Thajchayapong, P., Queener, S.F., Allen, D.O., and Bell, N.H. (1976). On the lipolytic action of parathyroid hormone in man. Metabolism *25,* 251-260.

Snijder, M.B., van Dam, R.M., Visser, M., and Seidell, J.C. (2006). What aspects of body fat are particularly hazardous and how do we measure them? Int. J. Epidemiol. *35,* 83-92.

Sorisky, A., Antunes, T.T., and Gagnon, A. (2008). The Adipocyte as a novel TSH target. Mini Rev. Med. Chem. *8,* 91-96.

Sorisky, A., Bell, A., and Gagnon, A. (2000). TSH receptor in adipose cells. Horm. Metab. Res. *32,* 468-474.

Steppan, C.M., Bailey, S.T., Bhat, S., Brown, E.J., Banerjee, R.R., Wright, C.M., Patel, H.R., Ahima, R.S., and Lazar, M.A. (2001). The hormone resistin links obesity to diabetes. Nature *409,* 307-312.

Stich, V., de Glisezinski, I., Galitzky, J., Hejnova, J., Crampes, F., Riviere, D., and Berlan, M. (1999). Endurance training increases the beta-adrenergic lipolytic response in subcutaneous adipose tissue in obese subjects. Int. J. Obes. Relat. Metab. Disord. *23,* 374-381.

St-Pierre, J., Lemieux, I., Perron, P., Brisson, D., Santure, M., Vohl, M.C., Despres, J.P., and Gaudet, D. (2007). Relation of the "hypertriglyceridemic waist" phenotype to earlier manifestations of coronary artery disease in patients with glucose intolerance and type 2 diabetes mellitus. Am. J. Cardiol. *99,* 369-373.

Stralfors, P., and Belfrage, P. (1985). Phosphorylation of hormone-sensitive lipase by cyclic GMP-dependent protein kinase. FEBS Lett. *180,* 280-284.

Subramanian, V., Garcia, A., Sekowski, A., and Brasaemle, D.L. (2004). Hydrophobic sequences target and anchor perilipin A to lipid droplets. J. Lipid Res. *45,* 1983-1991.

Suganami, T., Tanaka, M., and Ogawa, Y. (2012). Adipose tissue inflammation and ectopic lipid accumulation. Endocr. J. *59,* 849-857.

Sun, K., Kusminski, C.M., and Scherer, P.E. (2011). Adipose tissue remodeling and obesity. J. Clin. Invest. *121,* 2094-2101.

Surks, M.I., and Ocampo, E. (1996). Subclinical thyroid disease. Am. J. Med. *100,* 217-223.

Taggart, A.K., Kero, J., Gan, X., Cai, T.Q., Cheng, K., Ippolito, M., Ren, N., Kaplan, R., Wu, K., Wu, T.J.*, et al.* (2005). (D)-beta-Hydroxybutyrate inhibits adipocyte lipolysis via the nicotinic acid receptor PUMA-G. J. Biol. Chem. *280,* 26649-26652.

Taniguchi, A., Kataoka, K., Kono, T., Oseko, F., Okuda, H., Nagata, I., and Imura, H. (1987). Parathyroid hormone-induced lipolysis in human adipose tissue. J. Lipid Res. *28,* 490-494.

Tavernier, G., Barbe, P., Galitzky, J., Berlan, M., Caput, D., Lafontan, M., and Langin, D. (1996). Expression of beta3-adrenoceptors with low lipolytic action in human subcutaneous white adipocytes. J. Lipid Res. *37,* 87-97.

Taylor, S.S., Buechler, J.A., and Yonemoto, W. (1990). cAMP-dependent protein kinase: framework for a diverse family of regulatory enzymes. Annu. Rev. Biochem. *59,* 971-1005.

Thrush, A.B., Gagnon, A., and Sorisky, A. (2012). PKC activation is required for TSH-mediated lipolysis via perilipin activation. Horm. Metab. Res. *44,* 825-831.

Turer, A.T., Khera, A., Ayers, C.R., Turer, C.B., Grundy, S.M., Vega, G.L., and Scherer, P.E. (2011). Adipose tissue mass and location affect circulating adiponectin levels. Diabetologia *54,* 2515-2524.

Turer, A.T., and Scherer, P.E. (2012). Adiponectin: mechanistic insights and clinical implications. Diabetologia *55,* 2319-2326.

Unger, R.H., Clark, G.O., Scherer, P.E., and Orci, L. (2010). Lipid homeostasis, lipotoxicity and the metabolic syndrome. Biochim. Biophys. Acta *1801,* 209-214.

Vega, G.L., Adams-Huet, B., Peshock, R., Willett, D., Shah, B., and Grundy, S.M. (2006). Influence of body fat content and distribution on variation in metabolic risk. J. Clin. Endocrinol. Metab. *91,* 4459-4466.

Venkatakrishnan, A.J., Deupi, X., Lebon, G., Tate, C.G., Schertler, G.F., and Babu, M.M. (2013). Molecular signatures of G-protein-coupled receptors. Nature *494,* 185-194.

Wang, M., and Fotsch, C. (2006). Small-molecule compounds that modulate lipolysis in adipose tissue: targeting strategies and molecular classes. Chem. Biol. *13,* 1019-1027.

Watt, M.J., and Spriet, L.L. (2010). Triacylglycerol lipases and metabolic control: implications for health and disease. Am. J. Physiol. Endocrinol. Metab. *299,* E162-8.

Wei, F.Y., Nagashima, K., Ohshima, T., Saheki, Y., Lu, Y.F., Matsushita, M., Yamada, Y., Mikoshiba, K., Seino, Y., Matsui, H., and Tomizawa, K. (2005). Cdk5-dependent regulation of glucose-stimulated insulin secretion. Nat. Med. *11,* 1104-1108.

Welch, E.J., Jones, B.W., and Scott, J.D. (2010). Networking with AKAPs: context-dependent regulation of anchored enzymes. Mol. Interv. *10,* 86-97.

Wilkinson, K.D. (2005). The discovery of ubiquitin-dependent proteolysis. Proc. Natl. Acad. Sci. U. S. A. *102,* 15280-15282.

Wu, Z., Rosen, E.D., Brun, R., Hauser, S., Adelmant, G., Troy, A.E., McKeon, C., Darlington, G.J., and Spiegelman, B.M. (1999). Cross-regulation of C/EBP alpha and PPAR gamma controls the transcriptional pathway of adipogenesis and insulin sensitivity. Mol. Cell *3,* 151-158.

Zechner, R., Kienesberger, P.C., Haemmerle, G., Zimmermann, R., and Lass, A. (2009). Adipose triglyceride lipase and the lipolytic catabolism of cellular fat stores. J. Lipid Res. *50,* 3-21.

Zielke, A., Hoffmann, S., Plaul, U., Duh, Q.Y., Clark, O.H., and Rothmund, M. (1999). Pleiotropic effects of thyroid stimulating hormone in a differentiated thyroid cancer cell line. Studies on proliferation, thyroglobulin secretion, adhesion, migration and invasion. Exp. Clin. Endocrinol. Diabetes *107,* 361-369.

CURICULUM VITAE

SUMMARY OF QULAIFICATIONS

- B.Sc. Honours Biochemistry and Biotechnology, M.Sc Biochemistry (submitted)
- Additional two years equivalent lab experience (Chemistry and Biochemistry)
- Teaching experience (lecture and laboratory) at the university level
- Extensive community involvement including various leadership roles
- Excellent technical skills in Windows and Macintosh (Microsoft Word, Excel, PowerPoint, Internet search and literature review tools)
- Advanced English, Intermediate French and Beginner Spanish language skills

EDUCATION AND TRAINING

M.Sc. Candidate Biochemistry **2012-2014**
University of Ottawa, Ottawa, ON

B.Sc. Honours Biochemistry and Biotechnology **2008-2012**
Carleton University, Ottawa, ON

AWARDS, HONOURS, ACCOLADES

- Ontario Graduate Scholarship **2013-2014**
- NSERC Canadian Graduate Scholarship Masters Level **2012-2013**
- University of Ottawa Excellence Scholarship **2012-2014**
- Carleton University Highest Honours Graduate **2012**
- Carleton University Senate Medal **2012**
- NSERC Undergraduate Summer Research Award **2010-2011**
- Carleton University Dean's Summer Research Internship **2009**
- Carleton University Faculty of Science Scholarship **2008-2009**
- Carleton University Laurel Society Scholarship **2008-2012**

WORK EXPERIENCE

Teaching Assistant BCH3346 **2014**

- Biochemistry Laboratory II (University of Ottawa)
- In lab instruction, supervision and guidance during weekly lab sessions
- Report marking and collaboration with lab coordinator

Teaching Assistant BIOL2104 **2012**

- Introduction to Genetics (Carleton University)
- Running tutorials, responding to e-mails and holding office hours to answer students' questions

Summer Research Assistant **2009-2012**

- Stintzi Lab (2012): Effects of gut microbiota composition on *Campylobacter jejuni* pathogenesis and transcriptome
- Willmore Lab (2010 & 2011): Effects of PIAS3 on SUMOylation and phosphorylation of STAT3 transcription factor.
- Wang Lab (2009): Colormetric and near-infrared fluorescence turn-on molecular probe for direct and highly selective detection of cysteine in human plasma.

RESEARCH AND SCHOLARLY ACTIVITIES

Graduate studies M.Sc. Thesis Project (submitted) **2012-2014**
University of Ottawa, Ottawa, ON
- The Role of PRAJA2 in TSH- or isoproterenol-stimulated lipolysis in human adipocytes
- Presented at BMI poster day 2013, OHRI research day 2013 and BMI seminar day 2014

Undergraduate Honours Thesis Project **2011-2012**
Carleton University, Ottawa, ON
- DNA damage by anthropogenic (vehicle and industrial) exhaust
- Presented at undergraduate research day 2012

Publication in the Journal of Materials Chemistry **2010**
- Colorimetric and near-infrared fluorescence turn-on molecular probe for direct and highly selective detection of cysteine in human plasma. Wenhui Hao, Arran McBride, Skye McBride, Jian Ping Gao and Zhi Yuan Wang. *J. Mater. Chem.*, 2011, 21, 1040-1048.

COMMUNITY INVOLVEMENT

Global Brigades **2012-2014**
- VP medical/dental supplies (1yr), VP treasurer/ secretary and in-country leader (1yr)
- Participation in preparation and delivery of two week-long medical relief trips to rural Honduras
- Work in triage, consultation pharmacy and health education to locals

Roger's House **2012-2014**
- Assisting with respite care of children/youth diagnosed with life-limiting illnesses
- Working in a multi-disciplinary team, communicating with parents and family members

The Ottawa Hospital (Gastroenterology) **2012-2014**
- Maintaining a research database on patients' endoscopic ultrasound procedures

- Assisting with office work, shadowing procedures, data extraction from health charts and vOacis

Let's Talk Science **2012-2014**

- Organizing and presenting science lectures, demonstrations and hands-on experiments to youth in the classroom and at various community events

The Glebe Centre **2010-2012**

- Routine assistance to dementia patients, entertainment and contribution to a supportive environment

REFEREES

Dr. Alexander Sorisky, MD FRCPC

- University Chair, Division of Endocrinology and Metabolism (The Ottawa Hospital, University of Ottawa)

Dr. Avijit Chatterjee, MDCM MSc FRCPC

- Head of the Advanced Therapeutic Endoscopy Program, Division of Gastroenterology (The Ottawa Hospital)

Dr. William Willmore, PhD

- Associate Professor, Institute of Biochemistry (Carleton University)